

Chapter 13

Mapping and Interpretation of the Lithospheric Magnetic Field

Michael E. Purucker and David A. Clark

Abstract We review some of the controversial and exciting interpretations of the magnetic field of the earth's lithosphere occurring in the four year period ending with the IAGA meeting in Sopron in 2009. This period corresponds to the end of the Decade of Geopotential Research, an international effort to promote and coordinate a continuous monitoring of geopotential field variability in the near-Earth environment. One of the products of this effort has been the World Digital Magnetic Anomaly Map, the first edition of which was released in 2007. A second, improved, edition is planned for 2011. Interpretations of the lithospheric magnetic field that bear on impacts, tectonics, resource exploration, and lower crustal processes are reviewed. Future interpretations of the lithospheric field will be enhanced through a better understanding of the processes that create, destroy, and alter magnetic minerals, and via routine measurements of the magnetic field gradient.

13.1 Introduction

The magnetic field originating in the earth's lithosphere is part of the earth's magnetic field complex, a dynamic system (*Friis-Christensen et al. 2009*) dominated by the interaction of the earth's magnetic field dynamo with that of the sun's. The lithospheric field

is dominated by static (on a human time scale) contributions that typically represents less than 1% of the overall magnitude of the magnetic field complex, and originate from rocks in the crust and locally, the uppermost mantle. Interpretation of the lithospheric magnetic field is used in (1) structural geology and geologic mapping, and extrapolation of surface observations of composition and structure, (2) resource exploration and 3) plate tectonic reconstructions and geodynamics.

This article is designed as a review describing recent progress in mapping and interpreting the lithospheric magnetic field, and also includes some highlights from the 2009 IAGA meeting in Sopron, Hungary. Since IAGA meets every four years, we have designed this review to highlight progress in the four year period from 2005 through 2009, although references to earlier important works are not neglected, especially in the area of resource exploration. Several reviews bearing on the mapping and interpretation of the lithospheric magnetic field have appeared between 2005 and 2009. Review articles within books and encyclopedias have included those within the *Encyclopedia of Geomagnetism and Paleomagnetism* (Gubbins and Herrero-Bervera 2007) and the *Treatise of Geophysics* (Schubert 2007). The *Encyclopedia* included articles on the Crustal Magnetic Field (D. Ravat, pp. 140–144), Depth to Curie temperature (M. Rajaram, pp. 157–159), Magnetic anomalies for Geology and Resources (C. Reeves and J. Korhonen, pp. 477–481), Magnetic Anomalies, Long Wavelength (M. Purucker, pp. 481–483), Magnetic Anomalies, Marine (J. Heirtzler, pp. 483–485), and Magnetic Anomalies, modeling (J. Arkani-Hamed, pp. 485–490). The *Treatise of Geophysics* included articles on 'Crustal

M.E. Purucker (✉)

Raytheon at Planetary Geodynamics Lab, Goddard Space Flight Center, Code 698, Greenbelt, MD 20771, USA
e-mail: michael.e.purucker@nasa.gov

Magnetism' (Purucker and Whaler 2007), on the 'Source of Oceanic Magnetic anomalies and the geomagnetic polarity timescale' (Gee and Kent 2007) and on 'Plate Tectonics' (Wessel and Müller 2007). A series of workshops at the International Space Science Institute (Bern, Switzerland) in 2008 and 2009 on Planetary Magnetism (2008) and Terrestrial Magnetism (2009) has resulted in a review article on the earth's magnetic lithosphere (Langlais et al. 2010). Reviews in journals in this time frame include those of Nabighian et al. (2005), Mandea and Purucker (2005), and Robinson et al. (2008).

This review will highlight some of the controversial and exciting areas relating to the interpretation of the lithospheric magnetic field. We begin with the World Digital Magnetic Anomaly Mapping project (Korhonen et al. 2007), the first truly global compilation of lithospheric magnetic field observations. This sets the stage for the discussion of impact processes, and the magnetization and demagnetization processes involved. After briefly reviewing the magnetic record of terrestrial impact craters, we discuss recent quantitative and theoretical work in the area, both terrestrial and extra-terrestrial. We then go on to review some of the new interpretations at the Vredefort, Lonar, and Sudbury structures, with possible implications for the extraterrestrial record, especially at Mars. We next review some of the interpretations of magnetic data for tectonics, and structural geology and geologic mapping. Included within this section is recent work suggesting that parts of the uppermost mantle, especially in the vicinity of subduction zones, may be magnetic. If true, this may have important implications as a predictive tool for the spatial localization of large megathrust earthquakes and associated tsunamis. Following this is a review of interpretations for resource exploration, especially minerals, geothermal resources, and water. We also highlight some of the new developments in predictive mineral exploration models. This is followed by a review of the interpretation of lower crustal processes, motivated by exciting new work on ilmenite-hematite intergrowths by S. McEnroe and colleagues, and on the effects of pressure on magnetization by S. Gilder and colleagues.

13.2 World Digital Magnetic Anomaly Map

The first version of the World Digital Magnetic Anomaly Map (WDMAM), published by the Commission for the Geologic Map of the World (CGMW), summarizes our publicly available mapping knowledge of the lithospheric magnetic field of the Earth (Fig. 13.1) as of 2007. Prior to that compilation, there had been publicly available regional and continental scale digital compilations, and several global analog compilations. As befitting a subject with significant economic importance, commercial groups have also produced compilations for the exploration community. The digital data and metadata of the WDMAM are at 3 min of arc spacing, and 5 km above the WGS84 ellipsoid. They are available in grid and map form at <http://ftp.gtk.fi/WDMAM2007>. The map grew out of the peer review of several candidate models (Maus et al. 2007b; Hamoudi et al. 2007; Hemant et al. 2007). The NOAA model (Maus et al. 2007b) was selected as the base model, and subsequent changes were made to this base map prior to its publication as the WDMAM (Korhonen et al. 2007). Two versions of the WDMAM are available, A and B. The A version fills areas without near-surface data with a downward-continued CHAMP model (Maus et al. 2007a) whereas the B version uses model data derived from marine ages to fill in marine areas without near-surface data (Purucker et al. 2007). The B version is shown in the printed map available from the CGMW. The major data sets utilized for the WDMAM, their spatial resolution, and online links are available at <http://www.agu.org/pubs/eos-news/supplements/2007/25-263.shtml> and on the printed map. There are also a series of products derived from the WDMAM (equivalent source, Reduced to Pole, and analytic signal) that are available at <http://dapple.geosoft.com>. While the lithospheric field represented by the WDMAM may be quasi-static, the maps of that field continue to improve. Examples include a new full spectrum magnetic anomaly grid of the United States (Ravat et al. 2009), and a new global marine magnetic anomaly data set (Quesnel et al. 2009). We thus expect that there will be updates

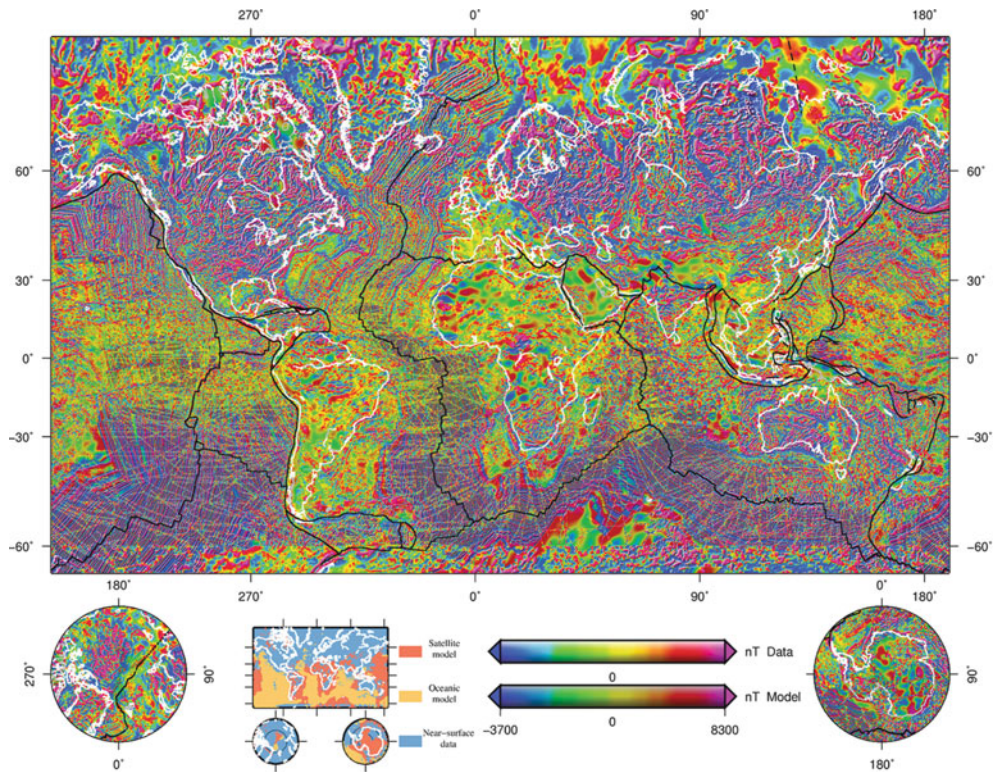


Fig. 13.1 Version B of the World Digital Magnetic Anomaly Map, with Mercator and polar stereographic projections, from Korhonen et al. (2007). The distribution of data sources is shown

in the index map. Ridges, fracture zones, and trenches are shown in black

to the WDMAM, with both formally released products from the WDMAM organization, and informal releases of interim products from individual research groups, such as the recent releases from NOAA at <http://geomag.org>. The next update is scheduled to be released in 2011.

13.3 Impacts

Impact cratering produces two classes of craters, the smaller 'simple' and the larger 'complex' (Melosh 1989). The two types can be distinguished based on their morphologies, and the transition between the two occurs at diameters of between 2 and 4 km on the Earth. Complex craters have central peaks, wall terraces, and a much smaller depth/diameter ratio than simple craters. They have undergone more collapse

than the simple craters, and the transition diameter is inversely proportional to the local (planetary) gravitational acceleration. At even larger diameters the central peak evolves into a central peak ring. Multi-ring craters are a type of complex crater characterized by multiple, large inward-facing scarps, and are most clearly developed on the Moon. Unlike the transition from simple to complex, or from complex to peak ring, multi-ring craters do not seem to scale with the local gravitational acceleration. The other crater type worthy of mention on the Earth is the 'inverted sombrero' often seen in km-size terrestrial craters and characterized by a disturbed central zone surrounded by a shallow moat. Atmospheric interactions may contribute to this distinctive shape, as discussed by Melosh (1989).

The magnetic signature of impact craters can be complex, but in general two types of features are often apparent (Pilkington and Hildebrand 2003).

Short-wavelength, relatively intense magnetic anomalies that occur near the center of the structure are the first of these types of features. Impact craters also disrupt the pre-existing magnetic signature, and that disruption is the second feature that can sometimes be recognized (Spray et al. 2004). The relatively intense magnetic anomalies occurring within the crater can be attributed to (1) uplifted magnetic lithologies, often basement, (2) magnetized impact melt rocks or breccia, (3) hydrothermal activity, (4) shock remanent magnetization or demagnetization, or (5) some combination of the above. Although variable, it is often the case that terrestrial impact structures are characterized by broad magnetic lows (Grieve and Pilkington 1996). Two useful guides to the variability of the magnetic signature are provided by the works of Ugalde et al. (2005), and Cowan and Cooper (2005). Numerical modeling using 2-D hydrocodes predict the distribution of pressure and temperature from which inferences can be made about the final magnetization distribution (Ugalde et al. 2005). While very useful, this model does not take into account later hydrothermal processes, which can significantly alter the magnetization distribution, and are often the source of significant ore deposits (Grant 1984; Clark 1997; Clark 1999).

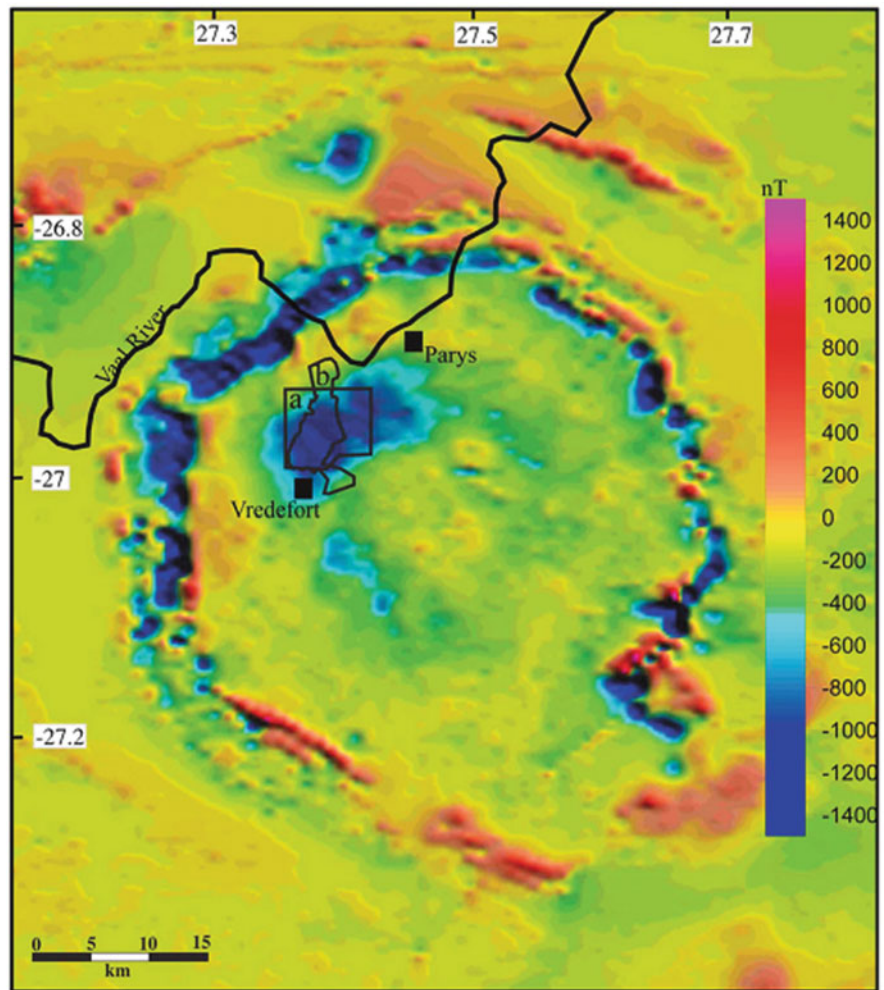
Recent work on the utility of the magnetic method over terrestrial impacts includes the work of Pilkington and Hildebrand on estimating the size of the transient and disruption cavity. These sizes can be directly related to the energy release associated with impact. Weak lower and upper bounds are placed on these quantities by establishing the sizes of two parameters: (1) the size of the relatively intense features in the interior of the crater, and (2) the size of the region where magnetic features have been disrupted. The authors suggest, based on 19 complex terrestrial structures, that the collapsed disruption cavity is about half the size of the crater diameter.

Of critical importance to the interpretation of the magnetic signature is the coherence scale, or size of a region of coherent magnetization (Lillis et al. 2010; Carporzen et al. 2005). The high-frequency and relatively intense magnetic features seen in the interior of impact basins, when upward-continued, often result in broad magnetic lows because adjacent coherently magnetized regions effectively cancel out. To complicate matters further, the coherence scale is often asymmetric. A simple example comes from the terrestrial oceans, where strongly magnetized sea-floor ‘stripes’

are often very narrow (kms) in a direction perpendicular to the spreading axis, but very wide (thousands of kms) in the direction parallel to the spreading axis. When marine magnetic surveys of the oceans are upward-continued to satellite altitude they ‘reveal’ that oceanic magnetic fields are much weaker than continental magnetic fields (Hinze et al. 1991). The reality is more complex. Typical oceanic basalts are much more magnetic than typical continental granitic rocks. Another example, discussed in depth below, comes from the Vredefort impact crater (Carporzen et al. 2005) where aerial measurements of the magnetic field are lower than over surrounding regions, but surface magnetizations from within the crater are large and variable on the cm scale. Finally, it should be noted that there may not be a single coherence scale for a particular region. The coherence scale is dictated by the physical process or processes at work, and multiple processes may result in multiple coherence scales. In certain idealized cases, it is often useful to employ the concept of a matched filter (Syberg 1972; Phillips 1997) to estimate the depths of the principal magnetic sources, and to estimate crudely what a map of the magnetic fields from those sources would resemble. Certain parameters are independent of coherence scale. Ideal body theory helps to establish bounds on quantities such as the magnetization strength required to explain a magnetic field distribution (Parker 1991; 2003, Purucker et al. 2009b).

The Vredefort impact in South Africa, Earth’s oldest and largest impact crater, has been the subject of several recent studies (Carporzen et al. 2005; Muundjua et al. 2007) and commentary (Dunlop 2005; Reimold et al. 2008; Muundjua et al. 2008). Carporzen et al. (2005) explain the elevated NRM intensities and Q-ratios typical of many of the exposed rocks at Vredefort as a consequence of short-lived plasmas produced during the impact. They find that paleomagnetic directions from the shocked but unmelted bedrock exposed to these hypothetical plasmas have directions which vary on scales of 10 cm or less. They explain the broad aeromagnetic low over the central portion of the impact (Fig. 13.2) as a consequence of viewing this spatially incoherent magnetic signal from an altitude of 150 m. Carporzen et al. (2005) also find magnetic evidence for lightning in the surface rocks at Vredefort, another example of a plasma phenomenon. According to the authors, lightning can reproduce many, but not all, of the magnetic features of the surface rocks. As

Fig. 13.2 Aeromagnetic anomaly map of the Vredefort impact structure, from Muundjua et al. (2007)



many as a quarter of their samples have been affected by lightning. Graham (1961) was the first to document the pervasive magnetic effects of lightning on surface rocks in South Africa. Carporzen et al. (2005) extrapolate their Vredefort results to the five youngest large impact basins on Mars (Lillis et al. 2010) where very weak magnetic fields have been measured. They suggest that a much smaller coherence wavelength characterized these basins, and the measured magnetic fields do not require the absence of a planetary dynamo when they were created. The Martian observations had previously been taken as evidence (Acuña et al. 1999) that these basins had been demagnetized by the impact, and that the magnetic dynamo had ceased by this time. In addition, it has been observed that the 14 oldest large impact basins on Mars have significant magnetic

fields associated with them (Lillis et al. 2008), suggestive of the presence of a magnetic dynamo at this time (Fig. 13.3). To explain the difference in terms of coherence wavelength, and not in terms of the presence or absence of a magnetic dynamo, suggests that another process is at work, perhaps changes in the aqueous alteration environment (Lillis et al. 2010).

The 1.85 Ga impact that produced the Sudbury structure struck a region of the southern Canadian shield characterized by late Archean and early Proterozoic faulting, and dike emplacement. Spray et al. (2004) document the termination of the magnetic signature of the 2.47 Ga Matachewan dike swarm as it reaches Ring 2 of the impact structure, some 65 km from the center of the impact (Fig. 13.4). Post impact magnetic dikes at 1.24 Ga are not terminated.

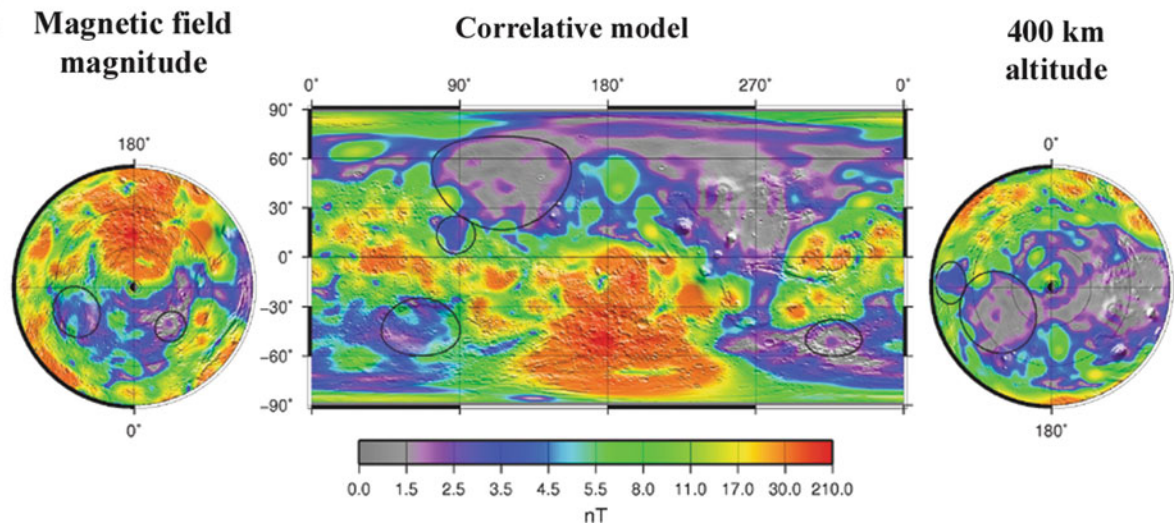


Fig. 13.3 Magnetic anomaly map of Mars, adapted from Lillis et al. (in press). The circles represent the visually determined locations of the youngest large impact basins on Mars

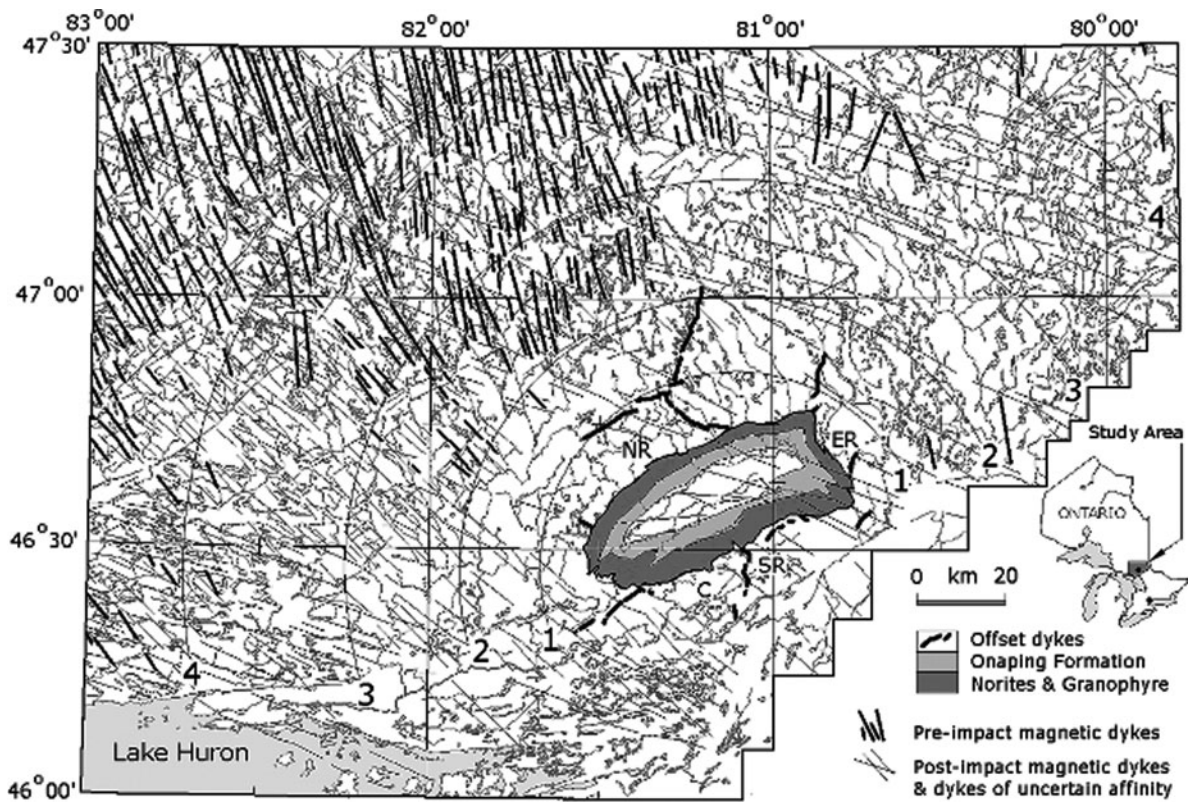


Fig. 13.4 Distribution of magnetic dikes, and ring structures, from Spray et al. (2004)

The authors interpret these observations in terms of shock demagnetization, and further interpret Ring 2 to correspond to a shock isobar pressure of between 1 and 10 GPa, depending on whether the magnetism of the dikes is dominated by induced or remanent magnetization.

A recent magnetic study of the Lonar impact structure (Louzada et al. 2008) documents the magnetic processes active at this simple, young (< 50 ka) crater formed in the Deccan basalts. In this 1.88 km diameter crater, shocked ejecta blocks exhibit a slightly elevated coercivity. No evidence of shock remanent magnetization (Gattacceca et al. 2008), shock demagnetization, or transient, plasma-related processes, such as have been suggested around larger impact structures, was identified.

13.4 Tectonics

Interpretations of magnetic field observations for tectonics, structural geology, and geologic mapping have a long history (Reeves 2007), and a recent special issue of *Tectonophysics* (Singh and Okuma 2009) highlights the utility of magnetic field observations in the understanding of complex crustal structure. The US Geological Survey has long been active in this area, and their current efforts include an ongoing program to evaluate seismic hazards in the Seattle (USA) region. The shallow earthquakes in this active forearc basin can be devastating, and paleoseismology studies indicate the presence of a M7+ earthquake some 1100 years ago on the Seattle fault, accompanied by a tsunami. Integrated magnetic studies (Blakely et al. 2002) have focused on recognizing these shallow faults, and tracing them in areas of poor exposure. Recent work in the Puget lowland (Sherrod et al. 2008) and to the west in the Olympic peninsula (Blakely et al. 2009) continues to unravel the complexities, and highlights the advances that can be made by an integrated geological and geophysical approach, which includes LIDAR, magnetics, gravity, and paleoseismological studies. For example, the Saddle Mountain deformation zone (Blakely et al. 2009) in the Olympic peninsula has been shown to have been active at approximately the same time as the Seattle fault, some 1100 years ago, suggesting a kinematic linkage between the two fault zones. The interpretation favored by the authors suggests that the Seattle and Saddle Mountain

zones form the boundaries of the northward advancing Seattle uplift.

Recent work (Blakely et al. 2005) suggests that parts of the uppermost mantle, especially in the vicinity of subduction zones, may be magnetic. At critical depths of 40 to 50 km, subducting ocean crust goes through important metamorphic changes that release large amounts of water into overriding mantle rocks. Introduction of water into the mantle produces serpentinite (Peacock et al. 2002), a highly magnetic, low-density rock (Fig. 13.5).

Thermal models (Oleskevich et al. 1999) indicate that, in many of the subduction zones of the world, this part of the mantle is cooler than the Curie temperature of magnetite, the most important magnetic mineral in serpentinite, and thus large volumes of mantle in subduction-margin settings should be magnetic. The World Digital Magnetic Anomaly Map (Fig. 13.6) does indeed show large-amplitude magnetic signatures over many of the world's subduction forearcs, including the Aleutian Islands, southern Alaska, Cascadia, Central America, and the Kurile Islands. Certainly these near-surface magnetic anomalies are caused in large part by upper crustal lithologies, and they have been recognized since the time of the U.S. satellite MAGSAT (Frey 1982). However, detailed analysis of a number of these subduction zones (Cascadia, Nankai, southern Alaska, Aleutians, and Central America) indicates that the magnetic anomalies also include long-wavelength components originating from mantle depths. These mantle-depth anomalies are thought to be caused by highly magnetic serpentinite in the mantle above the subducting slab (Blakely et al. 2005; Manea and Manea 2008).

Not all subduction zones exhibit high-amplitude magnetic anomalies, reflecting geothermal and geochemical complexities. Part of this may be the result of inadequacies in the WDMAM maps (Th ebault et al. in press), which form the background of several of the illustrations here. In the WDMAM, the oceanic component of the B map has been supplemented by models derived from the Digital Age map of the oceans, and the polarity reversal timescale. The details of both A and B maps, even in places where marine magnetic surveys have been conducted, are compromised by the inability to separate spatial from temporal variations, a consequence of the absence of base stations in marine magnetic surveys. Future generations of this map will result in a more objective and useful product.

Fig. 13.5 Highly simplified crust and upper mantle model of the Aleutian subduction zone and related serpentinite mantle wedge, showing predicted near-surface contributions of the wedge to magnetic and gravity anomalies

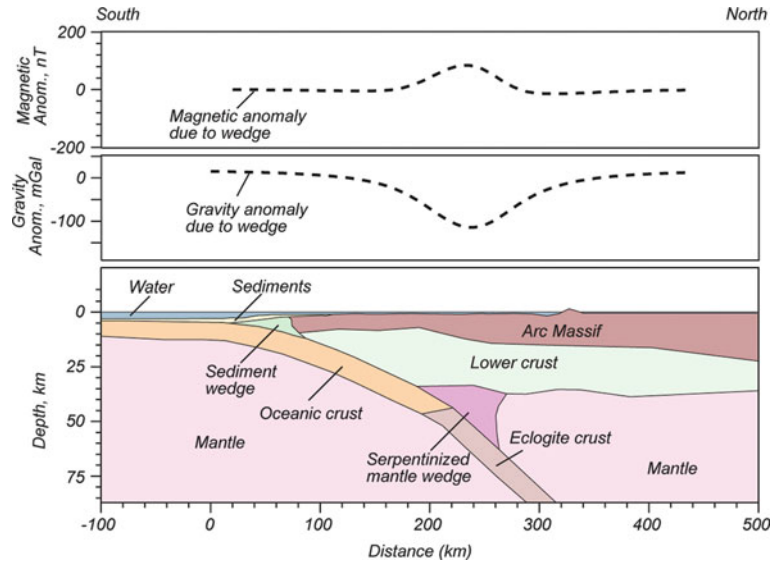
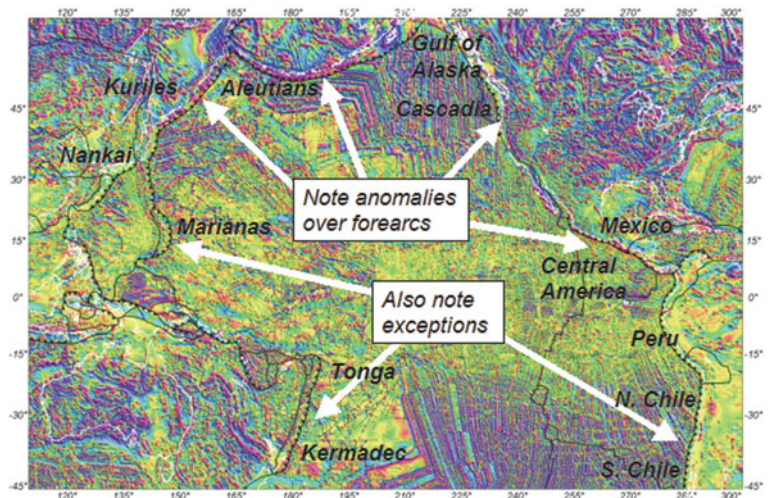


Fig. 13.6 Magnetic anomalies of the Circum Pacific, showing the location of subduction zone magnetic anomalies. Source: World Digital Magnetic Anomaly Map (Korhonen et al. 2007)



The presence of serpentinite in subduction margins has two important links to large and giant earthquakes, and associated tsunamis. First, dewatering the subducting slab is thought to embrittle the slab, reactivate pre-existing faults and other structures, and produce within-slab earthquakes (Kirby et al. 1996; Peacock et al. 2002). Thus, we expect to see a spatial association between this type of earthquake and mantle magnetic anomalies (Hyndman and Peacock 2003; Blakely et al. 2005). Second, in cool subduction margins, the down-dip limit of megathrust earthquakes (M 8.0–9.6) is controlled by the slab's first encounter with serpentinitized mantle (Oleskevich et al. 1999). Again, we

expect to see a spatial association between these devastating earthquakes and mantle magnetic anomalies. For example, the devastating 2004 and 2009 Sumatra-Andaman earthquakes are spatially associated with long-wavelength magnetic anomalies and thus consistent with the predicted pattern. Long recurrence intervals on megathrust earthquakes make current seismic compilations an unreliable guide to the location of past earthquakes, although non-volcanic tremors can be used, at least in part.

The existence of serpentinitized mantle is well demonstrated in a few subduction margins. At Cascadia, for example, anomalously low mantle

velocities have been interpreted as evidence for serpentinization of the mantle wedge (Bostock et al. 2002; Brocher et al. 2003), and these low-velocity zones are located directly beneath static long-wavelength magnetic anomalies (Blakely et al. 2005). However, in many of the subduction zones of the world, including the Aleutian Islands (Fig. 13.7), where a proposed magnetic survey (Serpent) would be conducted, seismic data appropriate for these studies are unavailable. If it can be demonstrated that long-wavelength magnetic anomalies are a reliable predictor of the presence of serpentinized mantle, then high-altitude magnetic surveys, such as the Serpent survey proposed to NASA by Purucker et al. (2009a) provide the promise of mapping hydrated mantle at subduction zones worldwide, thereby illuminating zones spatially and causally associated with both megathrust and within-slab earthquakes.

In the Antarctic, aeromagnetic surveys play a much larger role than elsewhere in deciphering tectonics because exposures of basement rocks are rare. The interpretation of a new survey over the Admiralty Block of the Transantarctic Mountains by Ferraccioli et al. (2009b) adds to our understanding of the relationships there between Cenozoic magmatism, faulting, and rifting. Fault zones here are defined by magnetic lineaments, and these help to define transtensional

fault systems which may have served to localize the McMurdo volcanics. Farther inland, interpretations of high-frequency aeromagnetic anomalies within the Wilkes subglacial basin (Ferraccioli et al. 2009a) suggest the presence of large volumes of Jurassic tholeiites which may be related to rifting. By analogy with the Cordillera of North America, the authors infer that the Wilkes basin contains fold and thrust belts and a former backarc basin. These features may represent the transition between the Precambrian East Antarctic craton and the Ross orogenic belt. On the other side of the Antarctic continent, Shepherd et al. (2006) delineated subglacial geology via a combined aeromagnetic and radio echo sounding survey over three tributaries of Slessor Glacier in the East Antarctic. They tentatively identified Jurassic dikes and sills intruding the Precambrian block here, and a post-Jurassic(?) sedimentary basin with a significant accumulation of sediment. Ice motion above the inferred sedimentary basin is seen to be different in character, comprising basal sliding and/or a deforming layer of sediment, than that above the remainder of the survey area.

In the Sinai peninsula, Rabeh and Miranda (2008) interpret a new high-resolution aeromagnetic survey, in conjunction with GPS and seismic data. They find systematic trends in the depth to the magnetic basement, and in the magnetically defined structural trends.

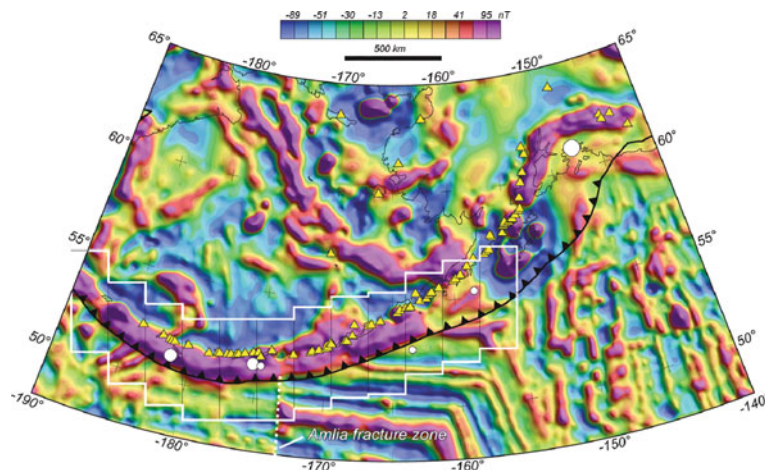


Fig. 13.7 Proposed high altitude Global Hawk magnetic surveys (Purucker and SerpentTeam 2010) over the Aleutian Islands and surrounding regions, outlined by the white polygon. Yellow triangles locate arc volcanoes, and white circles are historic megathrust earthquakes with magnitude greater than 8.0. The

Amlia fracture zone is indicated by the dotted white line. The color base map shows an approximation of magnetic anomalies observed at 20 km altitude. Anomalies were calculated by analytically continuing the World Digital Magnetic Anomaly Map to 20 km altitude, from its nominal 5 km altitude

The depth to basement increases to the west and north, reaching some 4 km deep at the north end of the study area.

Aeromagnetic, gravity, geologic, and remote sensing data were combined in the Eljufra region of Libya by Saadi et al. (2008) to define geologic structures and outline hydrothermally altered basalt. Analytic signal determinations of the magnetic field were used to estimate the location and depths of magnetic contacts.

Aeromagnetic surveys often provide unparalleled views of faults in sedimentary basins. For example, Grauch and Hudson (2007) find that prominent low-amplitude (5–15 nT) linear anomalies are often associated with surficially hidden faults that offset basin-fill sediments in the central Rio Grande rift of north-central New Mexico (USA). They also find that the linear anomalies are not the consequence of chemical processes acting within the fault zone, but rather due to the tectonic juxtaposition of magnetically different strata across the fault. They develop a set of simple graphical, mathematical, and conceptual models to help them determine parameters of direct interest to structural geology.

Drenth and Finn (2007) have also recognized hidden faulting in the Pine Canyon caldera of Big Bend National Park, along the US-Mexico border. The caldera-filling Pine Canyon rhyolite can be used as a magnetic marker because it is reversely magnetized. The authors use this marker to assess the thickness of the caldera fill, and suggest that it is controlled by buried faults evident in the magnetic survey.

Magnetic surveys, interpreted in conjunction with gravity and radiometric data, can also delineate basin architecture and tectonic evolution, as illustrated by the study of the Neocomian Rio do Peixe basin of NE Brazil (de Castro et al. 2007). The Rio do Peixe is a tripartite basin developed during the opening of the South Atlantic Ocean. Many pre-existing faults within the basement complex were reactivated during basin development, and the magnetics also serves to delineate the thickness of the sedimentary packages in these asymmetrical half-graben basins.

The utility of high-resolution airborne magnetic data in the interpretation of tectonic processes is borne out by the analysis of such a survey along a 120-km-long section of the Dead Sea Fault in Jordan and Israel (ten Brink et al. 2007). This fault is poorly delineated on the basis of surface morphology, or micro-seismic activity, although damaging earthquakes have struck

along this fault as recently as AD 1458. The fault is clearly seen on maps of the first vertical derivative, indicating a shallow source for the anomalies. The authors interpret these 5–20 nT anomalies as originating from the alteration of magnetic minerals due to groundwater within the fault zone. Based on modeling of the magnetic observations, the width of the shallow fault zone is several hundred meters wide. On a regional scale, the authors observe no igneous intrusions related to the fault zone, and confirm previous interpretations of 107–111 km of left-lateral offset across the fault.

Magnetic techniques continue to play a major role in delineating plate tectonic processes in the marine realm. Maia et al. (2005) document the interaction between the Foundation hotspot and the Pacific-Antarctic ridge within the South Pacific. Analysis of the magnetic anomaly data document a difference between the age of hotspot-related seamounts, and the underlying oceanic crust. This difference suggests that the ridge has approached the hotspot at a rate of 40 km Ma⁻¹. This is in good agreement with published radiometric dates.

13.5 Resource Exploration

Over the last three decades there have been dramatic improvements in the quality of magnetic surveys, accompanied by lowering of acquisition costs. Rapid developments in image processing, 3D visualization, computer-intensive enhancements of magnetic data and semi-automated interpretation methods have ensured that magnetic data is routinely acquired and used by geologists as well as geophysicists, at every stage of hard rock mineral exploration programs, from regional area selection to prospect scale exploration. Recognition of the information about the sedimentary section, as well as the crystalline basement, that is obtainable from modern high resolution magnetics has also led to greater use of magnetics in hydrocarbon exploration programs, although potential field methods will always remain subsidiary to seismic methods in that arena. Nabighian et al. (2005) have provided a comprehensive overview of the historical development of magnetics in exploration and the recent state of the art. Accordingly, we will concentrate on some new developments in magnetic exploration and some

hitherto unpublished work on magnetic signatures of mineralization.

Robinson et al. (2008) have reviewed magnetic and other geophysical methods for hydrogeological research, with suggestions for future research directions. Tectonic and structural interpretations derived from aeromagnetic and Landsat thematic mapper (TM) data sets form the basis for an ambitious program of groundwater exploration (Ranganai and Ebinger 2008) in the arid southern Zimbabwe craton (Africa). The lack of primary permeability and porosity in this crystalline basement terrain results in poor overall groundwater potential. However, available groundwater is localized by the presence of faults, fractures, dikes, and deeply weathered regions. These features are often recognizable through enhanced aeromagnetic and/or thematic mapper observations, and the authors utilize these to identify lineaments, and place them in the context of the regional structural geology. They develop a model in which the aeromagnetic data is used to map faults and fractures of considerable depth extent which may be open to groundwater (under tension) while the TM lineaments are typically closed to groundwater (under compression) and define recharge areas. The authors predict that coincident magnetic and TM lineaments, and continuous structures associated with large catchment basins, will be most favorable for groundwater. The sparse record of existing borehole data, some of which is of questionable quality, suggest a relationship between productivity and spatial proximity to faults and dikes, but proximity does not guarantee productivity. The trends of the NNE and NW sinistral faults in the Chilimanzi plutons can be traced from higher elevation areas in the north that represent the watershed, to lower areas in the arid south. Since regional groundwater flows mostly follow the dominant topographic gradient, these structures were identified as the most promising in terms of sustainable ground water resources.

Aeromagnetic data can also be utilized to infer heat flow within the crust, via determination of the depth to the Curie isotherm, the depth at which rocks lose their permanent and induced magnetism. When these determinations are from active geothermal areas, they provide important constraints on the depth to the heat source, and its extent. Espinosa-Cardena and Campos-Enriquez (2008) make such a determination from the Cerro Prieto geothermal area of NW Mexico. They find that the Curie point ranges from 14 to 17 km depth,

slightly deeper than previous studies, but supported by seismic, gravity, and heat flow measurements.

Province- and continental-scale compilations of magnetic data sets provide a useful framework for identifying regional crustal structures that control distribution of mineralization and favorable geological environments (e.g., Hildenbrand et al. 2000; Chernicoff and Nash 2002; Chernicoff et al. 2002; Betts et al. 2004; Sandrin and Elming 2006; Airo and Mertanen 2008; Austin and Mertanen 2008, 2009; Anand and Rajaram 2006; Anand et al. 2009), particularly if these data sets are integrated with other geophysical data.

By utilizing magnetic and gravity data in an integrated geological and geophysical study, Blakely et al. (2007) establish that the White River area of Washington exhibits many similarities to the Goldfield mining district of Nevada, home to one of the largest epithermal gold deposits in North America. To date, White River has produced only silica commercially, but deep weathering, young surficial deposits, and dense vegetation have hindered the evaluation of its economic potential for base and precious metals in the near surface. The magnetic data was invaluable in defining structural controls on hydrothermal alteration in both areas, but especially at White River because of poor exposures. The deposits are penecontemporaneous products of the Cascade Arc some 20 Ma ago. Gravity and magnetic data were instrumental in locating the intrusive body beneath both regions that presumably was the source of fluids and heat to the overlying calc-alkaline volcanic rocks. Magnetic susceptibility measurements at White River demonstrate the destruction of magnetic minerals in the altered rocks, and provide a way of estimating the depth extent of alteration (230–390 m). The White River altered area is located between two magnetically identified faults, in a temporary extensional stress regime.

Magnetic petrological studies of magnetic stratigraphy within layered intrusions (e.g., Ferré et al. 2009; McEnroe et al. 2009a) should improve detailed mapping within such intrusions, particularly beneath cover or between widely spaced drill holes, with evident applications to exploration for such commodities as Cr, PGEs, Ni, Cu, V and Ti.

The magnetic properties of igneous rocks that are genetically related to metalliferous mineralization vary systematically with the ore metals and deposit style (Clark 1999). Table 13.1 summarizes generalized

Table 13.1 Magnetic properties of Unaltered Weakly Altered Intrusive Rocks related to Mineralization

Lithology	Strongly Oxidized (NNO-HM)			Strongly Reduced (\leq QFM)		
	k (10^3 SI)	NRM	Associated mineralization	k (10^{-3} SI)	NRM	Associated mineralization
Syenogranite, Alkali granite	1–30	Weak, VRM, $Q < 1$	Mo, Mo-W, (Au)	0.1–0.3	V. weak, VRM, $Q \ll 1$	Sn, Sn-W
Monzogranite (Adamellite), Qtz monzonite	3–40	VRM, $Q < 1$	Cu, Cu-Mo, Au	0.1–0.4	V. weak, VRM, $Q \ll 1$	
Granodiorite, Monzonite, Tonalite	20–70	VRM, $Q < 1$	Cu, Cu-Mo, Cu-Mo-Au, Au	0.2–0.5	Weak; $Q \ll 1$	
Qtz diorite, Qtz monzodiorite	25–90	VRM + TRM; $Q < 1$	Cu-Au, Cu-Au-Mo, Au	0.4–0.6	Weak; $Q \ll 1$	
Monzodiorite, diorite	30–100	TRM+(VRM); $Q \sim 1$ ($Q < 1$)	Cu-Au, Au	0.5–0.8	Weak; $Q \ll 1$	
Gabbro, Norite, Alkali gabbro	40–160	TRM + (VRM); $0.5 < Q < 10$	Fe, Ti, V	0.6–1.3	Weak; $Q \ll 1$	Cr, PGEs

Rocks that have undergone deuteric alteration and/or minor rock-buffered hydrothermal alteration of normal type and intensity, as well as essentially unaltered rocks, are included here. Susceptibilities of unaltered and unmetamorphosed volcanic rocks are similar to those of their corresponding intrusive rocks, e.g., for a given igneous suite $k(\text{andesite}) \approx k(\text{diorite})$. NNO—HM indicates crystallization at oxygen fugacities between the Ni—NiO and hematite-magnetite buffers; \leq QFM indicates crystallization at oxygen fugacities at or below the quartz-fayalite-magnetite buffer. NRM = natural remanent magnetization, TRM = thermoremanent magnetization, VRM = viscous remanent magnetization, Q = Koenigsberger ratio.

results from a magnetic petrophysical database (Clark et al. 2004). Although for a given rock type the total range of susceptibilities given in Table 13.1 can be quite large, the general trends are clear. Within individual provinces, and in particular within specific igneous suites, the variability is much less. Understanding the magnetic signatures of magmatic-hydrothermal systems associated with mineralization requires detailed consideration of the effects of different alteration types on a range of protoliths. Some examples are given below.

Clark et al. (2004) produced a major study of the magnetic signatures of porphyry copper deposits, volcanic-hosted epithermal gold deposits, and iron-oxide copper-gold (IOCG) deposits. Although magnetic surveys are an integral part of exploration programmes for porphyry, epithermal and IOCG deposits, the magnetic signatures of these deposits and mineralized systems are extremely variable and exploration that is based simply on searching for signatures that resemble those of known deposits is rarely successful. However, the reasons for this variability are reasonably well understood and are summarized below.

A number of well-known geological models of porphyry and epithermal deposits are routinely used in exploration, even though most deposits fail to match the idealized models closely, due to post-emplacement tectonic disruption and rotations, asymmetric alteration zoning due to emplacement along a contact between contrasting country rock types, and so on. These complications are taken into account by exploration geologists as geological information about a prospect accumulates. The variability of magnetic signatures of these deposits reflects strong dependence of magnetic signatures on local geological setting, departures of real mineralized systems from idealized geological models, the direction and intensity of the geomagnetic field, which varies over the Earth, and differing magnetic environments (host rock magnetization, regional gradients, interference from neighbouring anomalies etc.). To tackle this problem Clark et al. (2004) developed the concept of predictive magnetic exploration models that are specific to the local geological environment and history, and are based on magnetic petrological principles (Clark 1997, 1999) applied to standard geological models, and on magnetic petrophysical data and detailed modeling

of selected deposits for which detailed magnetic and geological data are available.

Significant geological factors that affect magnetic signatures include tectonic setting and its influence on magma composition and mode of emplacement; influence of pre-existing structures on the geometry and depth of emplacement; and the crucial influence of host rock composition on alteration assemblages, including secondary magnetic minerals, and on the stability of primary magnetic minerals.

Magnetic signatures reflect not only the local geological setting at the time of emplacement, but also post-emplacement modification of deposits. Post-emplacement tilting of porphyry and epithermal systems and dismemberment by faulting are very common and drastically modify the geophysical signatures. Burial of a deposit by younger sedimentary or volcanic rocks also modifies the anomaly pattern. Conversely, exhumation and partial erosion of the system produces a very different magnetic signature. In older deposits, metamorphism can substantially modify the magnetic mineralogy of the deposits and host rocks, with concomitant changes in the magnetic anomaly pattern. Although the majority of porphyry and epithermal deposits are relatively young and, at most, weakly metamorphosed, some relatively ancient deposits in metamorphosed terrains are known. There is a strong possibility that some older porphyry and epithermal deposits occur that have not been recognized, because effects of metamorphism and deformation have obscured their true nature.

Given a comprehensive magnetic petrophysical database and the understanding of the geological factors that create and destroy magnetic minerals in porphyry systems, however, the magnetic effects of the above-mentioned geological complications are quite predictable. Variations in signatures due to varying geomagnetic inclination across the globe are best handled by calculating reduced-to-pole (RTP) signatures that can be compared with RTP processed survey data from high and moderate latitudes or in low latitudes, where RTP processing is unstable, by calculating reduced-to-equator (RTE) that can be compared with observed signatures, particularly if they are also reduced to the equator.

The porphyry copper model of Lowell and Guilbert (1970) has been highly influential in exploration programs and has been successfully applied in many different areas. It should be remembered, however, that

the model is based on a reconstruction of the San Manuel and Kalamazoo porphyry deposits in Arizona, which originally formed a single intrusion-centred orebody with concentric zoning, before being tilted and disrupted by faulting (Lowell 1968; Force et al. 1995). The present disposition of intrusive rocks and alteration zones in and around these orebodies differs greatly from the idealized model, but when the displacement along the San Manuel fault is removed and the intact porphyry system restored to the vertical, it is apparent that the system originally conformed closely to the model. Figure 13.8(a) shows a model of a Laramide type deposit, associated with a high sulfur quartz monzonite magma that intruded weakly magnetic felsic rocks and subsequently was tilted and dismembered by faulting in a similar fashion to the San Manuel-Kalamazoo system. The predicted magnetic signature is shown in Fig. 13.8(b)–(d). This model, and those in subsequent figures, were created using the *Noddy*TM structural history modeling program (Jessel 2001).

Such post-emplacement disruption of porphyry systems is common. Wilkins and Heidrick (1995) report that approximately 45% of the deposits of the southwestern North American porphyry copper province have been significantly faulted, extended and rotated during Oligocene and Miocene time. Tilting through more than 0° is common. Geissman et al. (1982) have quantified rotations in the Yerington district using paleomagnetism. A paleomagnetic study of the Porgera Intrusive Complex by Schmidt et al. (1997) showed that the upper levels of this complex have been disrupted by thin-skinned tectonics. The exposed intrusions have undergone substantial, but varying, degrees of tilting and rotation about vertical axes. Lum et al. (1991) point out the prevalence of local block rotations that distort outcrop patterns of high level intrusions and porphyry and epithermal alteration systems in the tectonically very active SW Pacific. Rotation rates of 20°–30° in 100,000 years are unexceptional.

A more straightforward modification of a zoned alteration system is afforded by the giant Chuquibambilla porphyry copper deposit in Chile (Lindsay et al. 1995), which has been bisected by a major fault, leaving a mineralized system with zoned alteration juxtaposed against unaltered intrusive rocks. Mineralized systems are susceptible to dismemberment, because major faults that controlled emplacement of intrusions and flow of hydrothermal

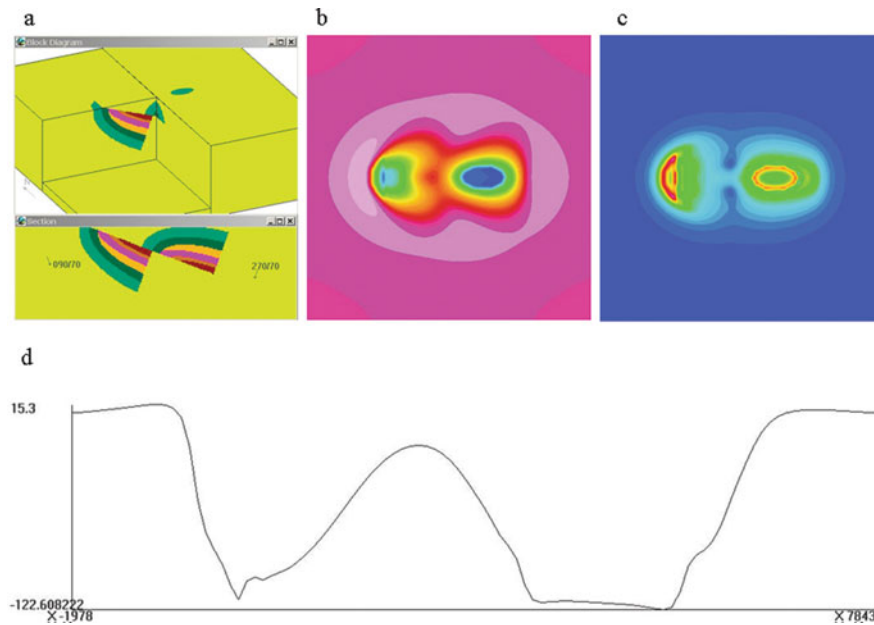


Fig. 13.8 (a) Laramide type quartz monzonite porphyry model with concentric zoning, emplaced vertically into felsic rocks and subsequently tilted and faulted. Alteration zones are inner potassic core (red), outer potassic (orange), ore shell (pink), phyllic/argillic (yellow), strong propylitic (dark green), and

weak propylitic (light green), (b) calculated RTP magnetic signature of model, (c) calculated analytic signal amplitude of RTP magnetic signature, (d) profile of calculated RTP magnetic signature across model

fluids, as at Chuquicamata, are often reactivated during or after deposition of mineralization.

Clark et al. (2004) summarized data from 50 deposits for which some information on magnetic signatures was available. The quality of the data is highly variable, making definitive statistical conclusions problematic. Taking the data at face value, however, they found that approximately 50% of deposits exhibited local RTP magnetic highs associated with mineralizing intrusions, approximately 70% had highs associated with alteration (usually potassic alteration with magnetite), approximately 70% also exhibited local magnetic lows over magnetite-destructive alteration zones, approximately 20% had highs associated with skarns, and 40–60% of deposits were associated with magnetic lineaments that appear to represent structural controls on mineralization. Recognition of structural controls, in particular, is very sensitive to the quality of the data. Many deposits show more than one of these features, accounting for the fact that the proportions add up to much more than 100%.

Of the deposits for which high resolution magnetic data are available, 12 show well developed concentric zoning patterns. Ten of these, the majority

from the Goonumbla cluster, New South Wales, have “doughnut” patterns, with central alteration low surrounded by an annular alteration high (Clark and Schmidt 2001). Two, the Bajo de la Alumbrera Cu-Au deposit and the Anabama Hill Cu prospect, have “archery target” patterns, with central alteration highs surrounded by annular alteration lows.

Although the number of well-characterized empirical examples of these types of zoned signature is low, the likely occurrence of similar signatures can be inferred from other information, e.g., the distribution of magnetite reported for some deposits. Predictive models are designed to bridge the gap between purely geological models (both idealized models and detailed deposit descriptions) and empirical magnetic signatures. This process has suggested the following conclusions for porphyry deposits that have not been significantly modified by post-emplacement tectonism or metamorphism:

- (i) The majority of gold-rich porphyry copper deposits (classic morphology, quartz-monzonite zoning pattern) hosted by magnetic mafic-intermediate volcanics are predicted to have

- large (> 1000 nT) bullseye high RTP anomalies over the potassic core, with incipient to prominent development of the archery target signature, depending on the extent of the phyllic zone, *providing erosion has exposed or nearly exposed the potassic zone*. This signature should be easily detectable beneath 100 m of sedimentary cover, and even beneath a similar thickness of magnetic volcanics.
- (ii) For a completely buried, uneroded or slightly eroded, gold-rich porphyry copper system the signature is basically an alteration low due to the large volume of magnetite-destructive alteration surrounding the deeply buried magnetic core. At intermediate levels of exposure a more complex pattern of a central high surrounded by an alteration low occurs, with the relative amplitude of the high and low dependent on the erosion level.
 - (iii) Similar deposits emplaced into weakly magnetic felsic rocks or unreactive rocks, such as quartzites or shales, are characterized by a strong bullseye high, without a surrounding low.
 - (iv) If emplaced into limestone the bullseye high associated with the potassically altered intrusion is likely to be supplemented by skarn anomalies (possibly remanently magnetized) associated with proximal magnetite-garnet skarn in favourable horizons, with discrete anomalies associated with distal skarn bodies, developed near the marble interface in structurally controlled zones. The skarn signature should be more strongly developed if the host rocks are dolomitic.
 - (v) Alkalic porphyry Cu-Au deposits typically exhibit diorite model zonation, with poorly developed phyllic zones, and produce strong bullseye highs over the potassic core.
 - (vi) In areas of greater crustal influence on magmas (e.g., the Laramide province), those magmas with relatively high sulphur content generate large volumes of magnetite-destructive alteration, in contrast to low sulfur magmas, for which magnetite is associated with potassic alteration. Porphyry Cu and Cu-Au deposits of the former type are associated with alteration lows, if emplaced into magnetic host rocks, or very weak signatures if emplaced into non-magnetic host rocks.
 - (vii) Giant porphyry copper deposits of the Atacama desert are characterized by large volumes of magnetite-destructive alteration, with locally developed magnetite-bearing potassic alteration, and thick overlying supergene blankets. The signature of such deposits, when hosted by moderately magnetic rocks, is an areally extensive alteration low, with a typical amplitude of approximately 100 nT. Such deposits will be visible to magnetics if they are covered by non-magnetic overburden, but cover by magnetic volcanics renders them difficult to see. When hosted by non-magnetic rocks the magnetic signature is inconspicuous, apart from local highs associated with remnant zones of potassic alteration within the broad zones of phyllic overprinting. These deposits are ringed by chargeable zones due to pyrite-bearing propylitic halos.
 - (viii) Phyllic alteration produced by magmatic, rather than meteoric, fluids (e.g., the Goonumbla, New South Wales, deposits) tends to be “inside-out” with respect to the potassic zone, producing a doughnut magnetic signature. Another source of this reverse zoning pattern may be structurally controlled access of meteoric fluids to deeper portions of a deposit. This type of signature is to be expected in two main settings: Volcanic morphological models, with small intrusive spines within comagmatic volcanics, tapped off a large mother magma chamber (e.g., Goonumbla), and plutonic/batholithic porphyry deposits.
 - (ix) Reduced porphyry Au-(Cu) and reduced intrusion-related gold deposits are characterized by incomplete doughnut signatures on a scale of kilometers, due to distal pyrrhotite-bearing mineralization developed in favourable sites, around a weakly magnetic intrusion.
- As an illustration of a specific category of predictive magnetic exploration model we will discuss gold-rich porphyry copper deposits, which have been intensively studied and for which genesis, structural controls, overall morphology and alteration zoning patterns are quite well understood (Sillitoe 2000).
- Predictive magnetic models for gold-rich porphyry copper deposits illustrated here conform to general geological models of this type of deposit and are closely based on deposits that may be regarded as archetypes for particular settings. In particular, the

Table 13.2 Canonical Magnetic Model of a Gold-Rich Porphyry Copper Deposit with a Magnetite-Rich Potassic Core, Hosted by Mafic-Intermediate Oxidized Igneous Rocks

Zone	Diameter* (m)	Width* (m)	Depth extent (m)	Susceptibility (SI)
Inner potassic	360	360	2400	0.351
Outer potassic	600	120	2500	0.173
Phyllic/argillic	1000	200	3000	0.003
Strong propylitic	1200	100	3000	0.007
Weak propylitic	1500	150	3000	0.027
Andesite/Basalt/Diorite/Gabbro	Very large	Very large	3000	0.043

*Diameters and widths of zones are maxima (at a depth 2000 m below the top of the phyllic zone for the propylitic and phyllic zones, and 1000 m below the top of the phyllic zone for the potassic zones).

model adopted for mafic-intermediate host rocks is based upon the Bajo de la Alumbrera deposit in Argentina (Guilbert 1995), and the model for carbonate host rocks is based upon Grasberg/Ertsberg (Papua New Guinea) (MacDonald and Arnold 1994; McDowell et al. 1996; Potter 1996). The assumed zoning is concentric with a magnetite-rich potassic core surrounded by a shell of phyllic alteration passing outwards into propylitic alteration (in silicate host rocks) or zoned skarn alteration (in a carbonate host).

The geometry of a gold-rich porphyry copper model, hosted by intermediate-mafic oxidized igneous rocks (nominally andesite), with a magnetite-rich potassic core is shown in Fig. 13.9(a). This type of model is mostly applicable to relatively mafic systems in island arc environments, or to those associated with alkaline (e.g., high-K calc-alkaline to shoshonitic) magmatism in continental settings. In Fig. 13.9(a) there has been insufficient erosion to expose the deposit. The top of the mineralization lies 500 m below the surface and the only sign of the mineralized system at the surface is a patch of propylitic alteration that could easily be overlooked or, if observed, assumed to be of little significance. The inner potassic zone is strongly mineralized and magnetite-rich. It is surrounded by an outer potassic zone that contains less abundant, but still significant, magnetite. The inner potassic zone represents relatively intense development of quartz-magnetite-K feldspar veins, whereas the outer potassic zone corresponds to biotite-K feldspar-quartz-magnetite alteration. A shell of magnetite-destructive phyllic alteration with very low susceptibility envelops the potassic zones. At upper levels this alteration may grade into intermediate argillic and shallow advanced argillic alteration, but the magnetic properties are equivalent for these alteration types and a single shell is sufficient to model the effects. The phyllic zone is surrounded

by a zone of intense propylitic alteration, which is partially magnetite-destructive, which passes out into weak propylitic alteration and then into unaltered andesite. The dimensions and susceptibilities of the zones are given in Table 13.2. The predicted reduced-to-pole (RTP) magnetic signature of this model is shown in Fig. 13.9b–c.

After 500 m of erosion (Fig. 13.9d) a patch of phyllic, surrounded by propylitic, alteration is exposed, but the mineralization is only subcropping. Removal of a 1 km thickness of rock exposes the mineralized core of the system and its surrounding alteration zones, as at Bajo de la Alumbrera.

An alternative model with lesser secondary magnetite is shown in Fig. 13.9g. Its RTP magnetic signature is shown in Fig. 13.9h–i. This model type is generally applicable to less strongly oxidized or relatively felsic systems, or to low-medium K calc-alkaline associations, typically in areas with thick continental crust.

Other models include deposits hosted by different country rocks, including weakly magnetic felsic igneous (or metaigneous) rocks, as shown in Fig. 13.9j–l, unreactive sedimentary rocks (e.g., quartzites), and carbonates. Quartzites (unaltered and within the propylitic and phyllic zones) and unaltered carbonates have essentially zero susceptibility.

The predicted RTP magnetic signatures for many deposit types depend strongly on the level of exposure. For exposed systems within magnetic intermediate-mafic igneous host rocks, as at Bajo de la Alumbrera, a strong central high is surrounded by a relatively weak annular low over the phyllic zone, gradually returning to background levels over the propylitic zone. For a completely buried system, however, the signature is basically an alteration low due to the large volume of magnetite-destructive alteration surrounding the deeply buried magnetic core. At intermediate

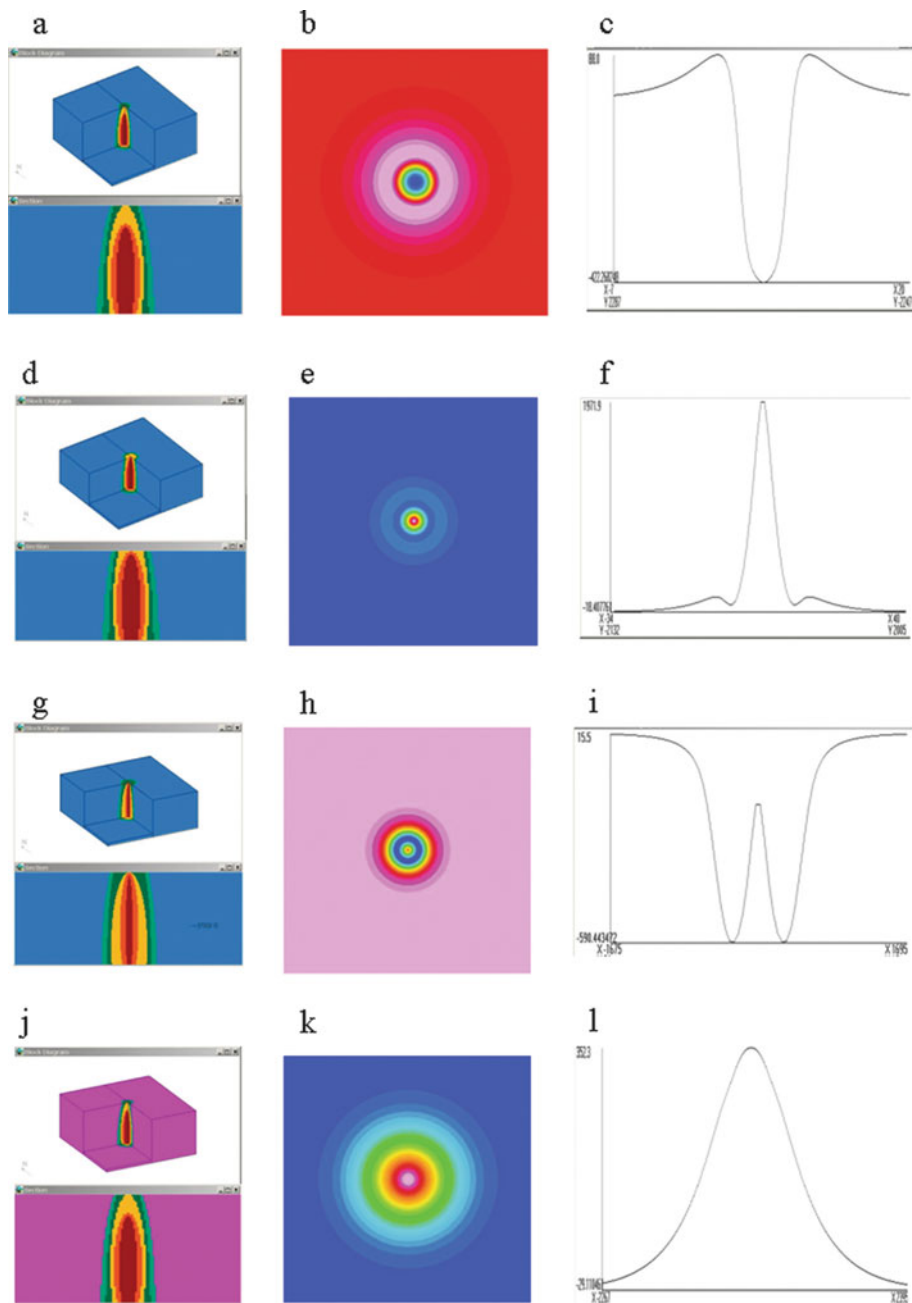


Fig. 13.9 Examples of canonical exploration models and their predicted magnetic signatures. (a) Gold-rich porphyry copper with magnetite-rich potassic core, emplaced into mafic-intermediate volcanics, uneroded, (b) RTP magnetic signature of model (a), (c) profile of RTP magnetic signature across model (a), (d) Same as model (a), with 500 m removed by erosion, (e) RTP magnetic signature of model (d), (f) profile of RTP magnetic signature across model (d), (g) As for model (a), with less

secondary magnetite in potassic core, (h) RTP magnetic signature of model (g), (i) profile of RTP magnetic signature across model (g), (j) Gold-rich porphyry copper with magnetite-rich potassic core, emplaced into felsic igneous rocks, uneroded, (k) RTP magnetic signature of model (j), (l) profile of RTP magnetic signature across model (j)

levels of exposure a more complex pattern of a central high surrounded by an alteration low occurs, with the relative amplitude of the high and low dependent on the erosion level.

For quartzites and similar host rocks, on the other hand, the signature is a simple high over the mineralized, potassically altered intrusion, for all levels of exposure. The anomaly becomes gradually weaker and broader with increasing depth of burial of the magnetic core. The signature for moderately magnetic felsic host rocks is intermediate between the signatures for mafic hosts and unreactive sedimentary host rocks, but the annular low around the central high is poorly developed, due to the relatively low magnetization contrast between the magnetite-destructive alteration zones (phyllic and strong propylitic) and the unaltered felsic rocks. Carbonate host rocks have the central high, with highs also developed over magnetite-rich proximal Cu-(Au) skarns, in the inner garnet-rich zone, and distal Au skarns, near the marble contact. These skarns tends to occur as discrete magnetite-bearing skarn bodies, developed within favourable horizons and localized by overall zonation patterns and by structural controls.

Figure 13.10a–c shows effects of burial under a significant thickness of magnetic volcanics of the deposit model shown in Fig. 13.9(a), demonstrating that such deposits should be clearly detectable beneath volcanic cover. Fig. 13.10d–f shows distortion of the magnetic signature produced by post emplacement tilting. Figure 13.10g–i illustrates a porphyry system similar to that of Fig. 13.9(a) but emplaced into carbonate rocks, and Fig. 13.10j–l shows the effects of asymmetric alteration zoning produced by emplacement into a contact between magnetic mafic rocks and carbonates.

With regard to epithermal gold deposits, intense epithermal-style alteration, whether low- or high-sulphidation, is invariably magnetite-destructive. The magnetic signature is strongly dependent on the host rocks. Epithermal alteration systems hosted by magnetic volcanic rocks are characterized by smooth, flat magnetic low zones within the overall busy magnetic texture (Irvine and Smith 1990, Feebrey et al. 1998). Similar systems within non-magnetic sedimentary rocks have negligible magnetic expression. High sulphidation systems may have a diffuse intrusion + alteration high due to a deeper porphyry system within a few hundred meters to a few kilometres of the deposit. This may be more prominent if post-formation

faulting has brought the intrusion closer to the surface, or the porphyry and epithermal systems are telescoped by rapid uplift during formation. Upward continuation of magnetic maps may help identify deep intrusions, beneath magnetic volcanics, that are possible sources for mineralizing fluids (Gunn et al. 2009). Magnetics can also be useful for detecting structural corridors and fluid pathways that are related to more localized epithermal systems. Radiometrics can detect K-rich alteration (e.g., adularia-sericite) associated with some exposed or subcropping epithermal deposits. Although in favourable circumstances magnetics is a useful tool for defining hydrothermal systems that are prospective for volcanic-hosted epithermal gold deposits, delineation of the ore zones is not possible. Electrical methods are generally more useful for detecting conductive or chargeable mineralization and defining resistive zones of silicification. Gravity methods are sometimes useful for defining lower density alteration, or in some cases enhanced density due to silicification of porous rocks.

Smith (2002) has reviewed geophysical signatures of IOCG deposits, with an emphasis on magnetics and gravity. Due to the high densities of iron oxide minerals, IOCG deposits are invariably associated with gravity highs, up to 20 mgal for large deposits. The magnetic signatures of IOCG deposits, and their relationships to the gravity anomalies, depend on the geological history and are much more variable. The iron oxide zonation pattern of IOCG systems (Hitzman et al. 1992; Wall and Gow 1995) indicates that the magnetic sources overall tend to be deeper and more laterally extensive than the gravity sources. For this reason detailed analysis of the anomalies should reveal a somewhat deeper and/or broader magnetic zone than the anomalous density distribution, as at the archetypical Olympic Dam, South Australia, deposit (Esdale et al. 2003). Thus a better term for the relationship between the magnetic and gravity anomalies is “superposed”, rather than “coincident”, anomalies.

Redox conditions during deposition and alteration overprinting, which controls the abundances and proportions of magnetite and hematite in IOCG deposits and their alteration envelopes are a crucial control on the magnetic signatures. Magnetite, formed under relatively reducing conditions, has very high susceptibility compared to hematite. Hematite has low susceptibility and also has fairly weak remanence, unless it has formed at, or been taken to, very high temperatures

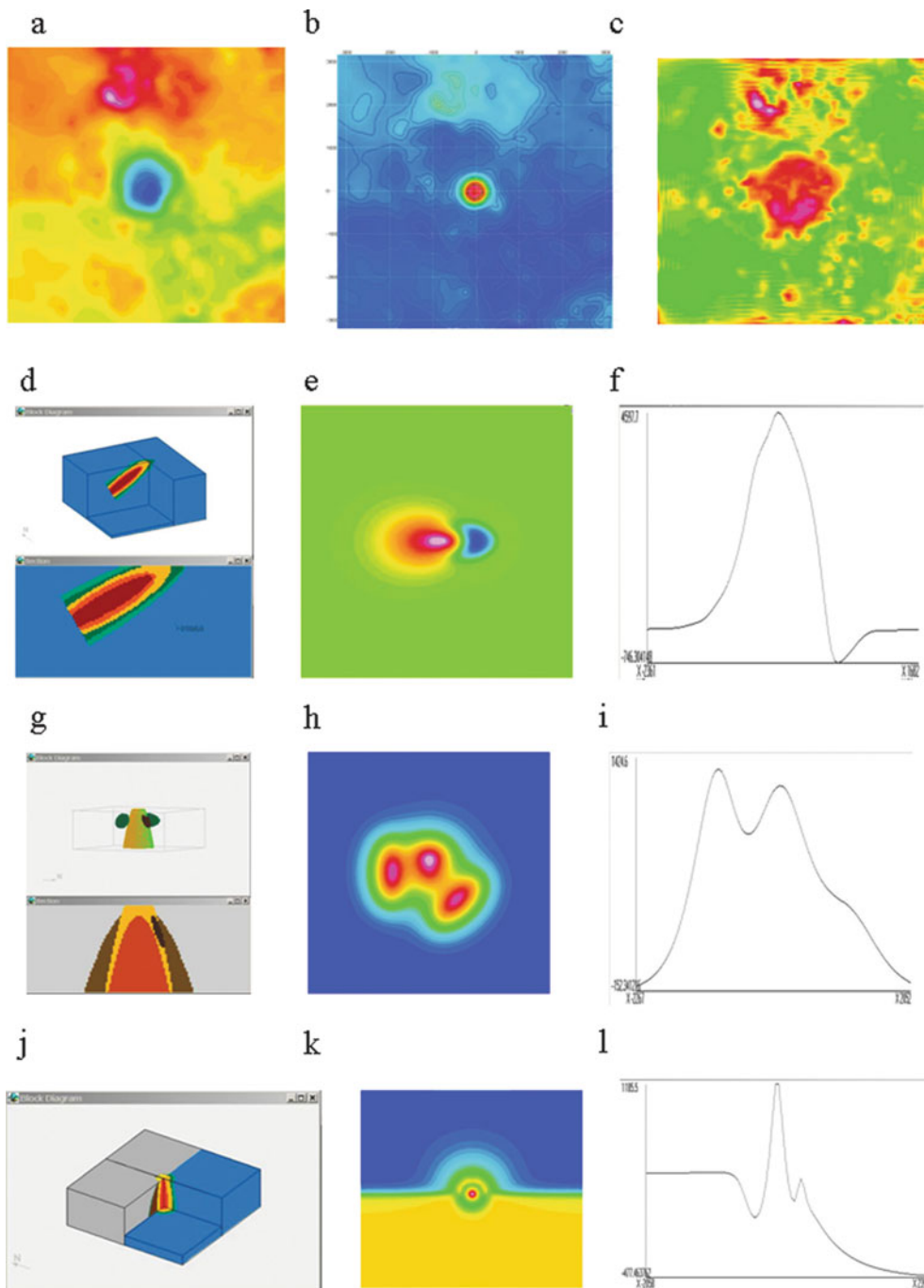


Fig. 13.10 Examples of canonical exploration models and their predicted magnetic signatures. (a) RTP magnetic signature of model in Fig. 13.9(a), buried beneath 100 m of magnetic volcanics (b) As for (a), but upper 1000 m of deposit removed by erosion, then covered by 100 m of magnetic volcanics (c) Analytic signal amplitude (total gradient) of RTP magnetic signature in (a), (d) Model of Fig. 13.9(a), with post-formation tilt through 60 degrees, (e) RTP magnetic signature of model (d), (f) profile of RTP magnetic signature across model (d),

(g) Gold-rich porphyry copper, emplaced into carbonate rocks with magnetite-rich potassic core plus proximal and distal skarns, eroded 500 m, (h) RTP magnetic signature of model (g), (i) profile of RTP magnetic signature across model (g), (j) Gold-rich porphyry copper with magnetite-rich potassic core, emplaced into contact between mafic volcanics and carbonate rocks, eroded 500 m, (k) RTP magnetic signature of model (j), (l) profile of RTP magnetic signature across model (j)

and thereby acquired a thermoremanent magnetization. Monoclinic pyrrhotite, formed under reducing conditions with moderate sulphur fugacity, has moderate susceptibility, but tends to carry intense remanence. The oxidation state of the host sequence appears to influence the oxidation state of the IOCG deposits, as well as the redox state of the source (e.g., magmatic fluids) and the paleodepth (more oxidized at shallow depths). IOCG deposits tend to occur in relatively oxidized crustal provinces, characterized by strong anomalies and complex magnetic patterns (Haynes 2000). Within the regional magnetic variability, the deposits lie within or near relatively strong magnetic highs, associated with semi-regional magnetite-producing sodic and sodic-calcic alteration systems.

In a typical vertically zoned IOCG system, magnetite-destructive, hematite-rich hematite-sericite-chlorite-carbonate (HSCC) alteration dominates upper levels, whereas magnetite-rich alteration (potassic at intermediate depths, grading into deeper sodic or sodic-calcic alteration) dominates at depth. Thus the current erosion level determines whether the exposed or near-surface portions of the system are hematite-rich or magnetite-rich. If the level of exposure is sufficiently deep, overprinting magnetite-rich potassic alteration tends to be more focussed around the deposits, enhancing the magnetic highs. On the other hand, if upper levels of the system have been retained, magnetite-destructive hematite-rich alteration hosts the mineralization. In this case the signature is a relatively smooth pattern, which can be a local magnetic low (depending on the host rock magnetization) within the overall broad high associated with deeper and/or more laterally extensive magnetite-dominant alteration. Tilting of a vertically zoned system, or upfaulting of the deeper magnetite-rich portion, may juxtapose the magnetite and hematite zones, producing juxtaposed, rather than “coincident” gravity and magnetic anomalies.

High grade regional or contact metamorphism of hematite-rich zones can impart an intense thermoremanence to the hematite, which can cause large magnetic anomalies. This appears to explain the strong magnetic anomalies exhibited by massive hematite bodies of the Mount Woods Inlier that have been contact metamorphosed, such as the Peculiar Knob deposit (Schmidt et al. 2007), whereas similar unmetamorphosed massive hematite at Prominent Hill produces no discernible magnetic anomaly.

At continent to province scale favourable tectonic settings for ancient deposits may be recognisable from regional potential field data sets, supplemented by seismic, magnetotelluric or other deep-penetrating methods. Ancient buried subduction zones are characterized by arc-parallel linear belts of magnetic highs, corresponding to magnetite-series granitoid provinces, and lows, corresponding to ilmenite-series granitoid provinces or sedimentary basins. Subduction-related magnetite-series belts are much more prospective for IOCG and porphyry copper-(gold) deposits. Belts of reduced, ilmenite-series granitoids are prospective for Sn-(W) and also for intrusive-related Au and reduced porphyry Au-(Cu) deposits. Within belts of magnetite-series granitoids, Cu-Au is associated with more magnetic magmatic-hydrothermal systems than Cu-Mo; W-Mo-Bi and Au in tin provinces is much less magnetic. In oxidized Au-bearing systems, Au mineralization is often associated with the felsic end of magmatic evolution and is then associated locally with a weaker magnetic character and higher radioelement contents. Continental rift settings, which are also prospective for IOCG deposits, may be associated with rift-parallel regional gravity and magnetic highs along the ancient continental margin, with a quiet magnetic zone outboard of the regional highs and relatively busy magnetic patterns inboard of the margin (Gunn 1997). Large intrusions associated with bimodal magmatism, which is characteristic of anorogenic environments, including several IOCG provinces, can be seen in magnetic and gravity images, due to the contrasting physical properties of mafic and felsic intrusions.

At a regional scale major structures that control the emplacement of mineralizing or heat-engine magmas, or which channel flow of crustal fluids, are often evident in suitably processed gravity and magnetic data sets (e.g., Sandrin et al. 2007). These features may also be visible in satellite imagery. Intersections of lineaments appear to be particularly favourable for IOCG mineralization. Structural controls at a range of scales, from semiregional to prospect scale, may be evident in detailed magnetic data. Identification of favourable orientations of structures may be possible if senses of movement, block rotations etc. are known. Anomaly offsets and abrupt changes of trend in magnetic images can help to define tectonic movements. Paleomagnetic studies can also be useful for defining rotations and tilting within and around deposits (Geissman et al.

1982; Force et al. 1995; Schmidt et al. 1997) and to define distinct magmatic and hydrothermal alteration events recorded by remanent magnetization (Schmidt et al. 1997; Clark and Lackie 2003; Astudillo et al. 2010).

A large range of magma compositions within a comagmatic suite is indicative of substantial fractional crystallization, which can partition metals into late stage fluids, potentially concentrating them to levels that can produce economic ore deposits. For this reason fractional crystallization is favourable for development of intrusive-related mineralization. Strongly zoned oxidized intrusions produced by fractional crystallization exhibit zoned magnetic signatures and, if exposed or subcropping, zoned radiometric patterns. Similarly, multiple/nested intrusions, with a substantial range of magnetic properties, densities and radioelement contents, particularly when there are geophysical indications of an underlying magma chamber, are also favourable indicators of fractional crystallization.

Well-developed contact aureoles around intrusions are indicative of emplacement of high-temperature, melt-rich magma capable of undergoing substantial fractional crystallization. Strong contact aureole effects produce substantial mineralogical changes in the metamorphosed and metasomatized host rocks, often with pronounced changes in magnetic susceptibility (particularly increased susceptibility due to creation of secondary magnetite and/or pyrrhotite). Strong remanent magnetization of contact aureoles is also suggestive of high temperature emplacement or substantial metasomatism. Prominent contact aureole magnetic signatures, particularly if they are clearly zoned or show strong local overprinting are therefore also favorable indicators of potentially mineralized magmatic-hydrothermal systems.

Future advances in magnetic exploration will rely firstly on better understanding of the processes that create, destroy and alter magnetic minerals in mineralized environments, based on magnetic petrological studies, accompanied by more comprehensive magnetic property databases and detailed case studies of magnetic signatures of mineralized environments. Secondly, improvements in acquisition, processing and interpretation of the crustal magnetic field will enable more geological information to be extractable from magnetic surveys. Although small incremental improvements in conventional surveys will continue, the most dramatic advances are likely to involve gradiometry,

particularly measurements of the full gradient tensor by new generation highly sensitive instruments, to obtain more detailed information about structures and subtly varying magnetization patterns in the shallow crust.

In a seminal paper Pedersen and Rasmussen (1990) discuss in some detail the practical problems encountered in the collection and processing of gradient tensor data and the benefits obtainable from acquisition of tensor data. For instance, these workers point out that resolution is enhanced compared to conventional magnetic surveys and that rotational invariants calculated from tensor data have attractive properties for interpretation. Christensen and Rajagopalan (2000) suggested that the next breakthrough in magnetic exploration is likely to be the measurement of the gradient tensor and demonstrated the utility of analytic signal amplitudes (total gradients) of vector components, which can be derived directly from gradient tensor components, for locating boundaries and interpreting source geometries in the presence of remanence. Schmidt and Clark (2006) have summarized the multiple benefits of gradiometry in general and tensor gradiometry in particular.

Recently the first practical low temperature (liquid helium cooled) SQUID-based system for geophysical gradient tensor surveys has been developed by the Jena (Germany) group (Stolz et al. 2006). The intrinsic noise of the LTS planar gradiometers developed by this group is 0.2 pT m^{-1} (integrated between 0.01 Hz and 10 Hz). Noise spectral density of the full tensor gradiometer system in motion is about $1\text{--}10 \text{ pT m}^{-1}(\sqrt{\text{Hz}})^{-1}$ over a frequency range of 0.1–2 Hz in a bird towed beneath a helicopter and approximately ten times higher for installation on a fixed wing aircraft.

The discovery of high temperature (liquid nitrogen temperatures and above) superconducting materials in the late 1980s has created opportunities for cheaper, smaller devices that can be readily transported and refilled, but retain very high sensitivities. Liquid nitrogen cooled SQUIDs and gradiometers are very sensitive, with noise levels that are about an order of magnitude higher than those of low T SQUIDs. Clark et al. (1998) suggested the use of combined vector field and gradient tensor measurements, using high T superconducting devices, for separating contributions of induced and remanent magnetization to magnetic anomalies and for inferring source properties, such as

total magnetization direction, remanence direction and Koenigsberger ratio.

A number of tensor gradiometer systems, based on a wide range of different technologies including high temperature SQUID devices, are under development (e.g., Clem et al. 2001; Humphrey et al. 2005; Leslie et al. 2007; Wiegert et al. 2007; Sunderland et al. 2009; Keenan et al. 2010). We anticipate that over the next decade full gradient tensor systems will be commercialized and be routinely used in next generation magnetic surveys for exploration.

13.6 Interpretation of Lower Crustal Processes

Lower crustal processes are dominated by increasing temperatures, and an important temperature is that associated with the Curie point of magnetite (580°C), above which it loses its permanent and induced magnetism. To the extent that other magnetic minerals dominate in the lower crust, the temperatures of those other magnetic phases will be important for interpretation. Ilmenite-hematite, hematite-magnetite, or titanomagnetite-rich, phases exhibit different Curie, Néel, or unblocking temperatures from pure magnetite (McEnroe et al. 2004), and they extend to 670°C for hematite-rich compositions. Fine-scale exsolution of ilmenite-hematite phases (McEnroe et al. 2009b), and possibly also magnetite-hematite phases (Schmidt et al. 2007), significantly increases the magnetic remanence and coercivity from typical multi-domain values. If these lamellae are not resorbed by temperature and pressure conditions in the lower crust, then a much greater range of magnetic mineral phases may be present. Experiments by McEnroe et al. (2004) suggest that the lamellae may be stable at lower crustal temperatures and pressures.

Increasing pressures also have an effect on the magnetic properties of single and multi-domain magnetite (Gilder et al. 2004) and titanomagnetite (Gilder and Le Goff 2008). Both saturation remanent magnetization and coercivity increase markedly in titanomagnetites at typical lower crustal pressures. The percentage of Ti in the titanomagnetite structure seems to control the increase in magnetization and coercivity, with the highest increases associated with the highest amounts of Ti.

Much work continues to be devoted to the difficult question of determining the depth to the Curie and Néel isotherms, and with comparing results from different approaches. Works utilizing standard approaches (Spector and Grant 1970) include those of Bilim (2007), Bektas et al. (2007), and Maden (2009) in Turkey, Trifonova et al. (2009) in Bulgaria, ChunFeng et al. (2009) and Xu-Zhi et al. (2006) in China, Prutkin and Saleh (2009) in Egypt, and Stampolidis et al. (2005) in Albania. A fractal approach based on the formulation of Maus et al. (1997) was used in the western United States by Bouligand et al. (2009), and a similar approach was used in California by Ross et al. (2006). Ravat et al. (2007) compares several spectral approaches, while Rajaram et al. (2009) compares the spectral approach with an approach that integrates seismic, heat flow, and satellite magnetic data sets (Purucker et al. 2007).

13.7 Summary

The interpretation of terrestrial impact structures continues to garner much attention because of its relevance to the interpretation of extraterrestrial impacts. These impacts are the targets of robotic exploration by NASA, ESA, and the national space agencies of Japan, India, and China.

The importance of the coherence scale, or size of a region of coherent magnetization, can not be overemphasized, both in the terrestrial and extraterrestrial examples. It is often the case that observations of a feature are made from only a single altitude. A change in that altitude can often make a dramatic difference in what features are available for interpretation, and ‘color’ the interpretation in subtle ways.

Future advances in magnetic exploration are critically dependent on a better understanding of the processes that create, destroy, and alter magnetic minerals. Comprehensive magnetic property databases are also a requirement for future advances in magnetic exploration.

The magnetic technique has often been faulted as having too little resolution. Recent advances in the measurement, processing, and interpretation of gradient data utilizing high temperature SQUID devices on helicopters and fixed-wing aircraft offer the prospect of dramatic improvements in the resolution of our

magnetic imagery. Similar improvements in our view of the magnetic lithosphere from near-Earth space will be inaugurated with the Swarm constellation (Friis-Christensen et al. 2009). Swarm will utilize highly sensitive Helium and fluxgate magnetometers flying in constellation to make its gradient field measurements.

Acknowledgments We would like to acknowledge the support of the SERPENT proposal team, especially R. Blakely (USGS) for Fig. 13.5, Fig. 13.6, and Fig. 13.7 and R. Bracken (USGS) for Fig. 13.7.

References

- Acuña M et al (1999) Global distribution of crustal magnetization discovered by the Mars global surveyor MAG/ER experiment. *Science* 284(5415):790–793
- Airo M, Mertanen S (2008) Magnetic signatures related to orogenic gold mineralization. *J Appl Geophys* 64:14–24
- Anand S, Rajaram M (2006) Aeromagnetic data analysis for the identification of concealed uranium deposits: a case history from Singhbhum uranium province, India. *Earth Planet Space* 58:1099–1103
- Anand S, Rajaram M, Majumdar T, Bhattacharyya R (2009) Structure and tectonics of 85 E Ridge from analysis of geopotential data. *Tectonophysics* 478:100–110
- Astudillo N, Roperch P, Townley B, Arriagada C, Chauvin A (2010) Magnetic polarity zonation within the El Teniente copper-molybdenum porphyry deposit, central Chile. *Mineralium Deposita* 45:23–41
- Austin J, Blenkinsop T (2008) The Cloncurry Lineament: Geophysical and geological evidence for a deep crustal structure in the eastern succession of the Mount Isa Inlier. *Precambrian Res* 163:50–68
- Austin J, Blenkinsop T (2009) Local to regional scale structural controls on mineralization and the importance of a major lineament in the eastern Mount Isa Inlier, Australia: review and analysis with autocorrelation and weights of evidence. *Ore Geol Rev* 35:298–316
- Bektas O, Ravat D, Bueyueksarac A, Bilim F, Ates A (2007) Regional geothermal characterisation of East Anatolia from aeromagnetic, heat flow and gravity data. *Pure Appl Geophys* 164(5):975–998. doi:10.1007/s00024-007-0196-5
- Betts P, Barraud J, Lumley J, Davies M (2004) Aeromagnetic patterns of half-graben and basin inversion: implications for sediment-hosted massive sulfide Pb-Zn-Ag exploration. *J Struct Geol* 26:1137–1156
- Bilim F (2007) Investigations into the tectonic of Kutahya-Denizli region, lineaments and thermal structure western Anatolia, from using aeromagnetic, gravity and seismological data. *Phys Earth Planet Inter* 165(3–4):135–146. doi:10.1016/j.pepi.2007.08.007
- Blakely R, Wells R, Weaver C, Johnson S (2002) Location, structure, and seismicity of the Seattle fault zone, Washington: evidence from aeromagnetic anomalies, geologic mapping, and seismic-reflection data. *Geol Soc Am Bull* 114(2):169–177
- Blakely R, Brocher T, Wells R (2005) Subduction-zone magnetic anomalies and implications for hydrated forearc mantle. *Geology* 33(6):445–448. doi:10.1130/G21447.1
- Blakely RJ, John DA, Box SE, Berger BR, Fleck RJ, Ashley RP, Newport GR, Heinemeyer GR (2007) Crustal controls on magmatic-hydrothermal systems: A geophysical comparison of White River, Washington, with Goldfield, Nevada. *Geosphere* 3(2):91–107. doi:10.1130/GES00071.1
- Blakely RJ, Sherrod BL, Hughes JF, Anderson ML, Wells RE, Weaver CS (2009) Saddle mountain fault deformation zone, Olympic Peninsula, Washington: western boundary of the Seattle uplift. *Geosphere* 5(2):105–125. doi:10.1130/GES00196.1
- Bostock M, Hyndman R, Rondenay S, Peacock S (2002) An inverted continental Moho and serpentinization of the forearc mantle. *Nature* 417(6888):536–538
- Bouligand C, Glen JMG, Blakely RJ (2009) Mapping Curie temperature depth in the western United States with a fractal model for crustal magnetization. *J Geophys Res Solid Earth* 114. B11104, doi:10.1029/2009JB006494
- Brocher T, Parsons T, Trehu A, Snelson C, Fisher M (2003) Seismic evidence for widespread serpentinized forearc upper mantle along the Cascadia margin. *Geology* 31(3):267–270
- Carporzen L, Gilder S, Hart R (2005) Palaeomagnetism of the Vredefort meteorite crater and implications for craters on Mars. *Nature* 435(7039):198–201. doi:10.1038/nature03560
- Chernicoff C, Nash C (2002) Geological interpretation of Landsat TM imagery and aeromagnetic survey data, northern Precordillera region, Argentina. *J South Am Earth Sci* 14:813–820
- Chernicoff C, Richards J, Zappettini E (2002) Crustal lineament control on magmatism and mineralization in northwestern Argentina: geological, geophysical and remote sensing evidence. *Ore Geol Rev* 21:127–155
- Christensen A, Rajagopalan S (2000) The magnetic vector and gradient tensor in mineral and oil exploration. *Preview* 77
- ChunFeng L, Bing C, ZuYi Z (2009) Deep crustal structures of eastern China and adjacent seas revealed by magnetic data. *Sci China Series D Earth Sci* 52(7):984–993. doi:10.1007/s11430-009-0096-x
- Clark D (1997) Magnetic petrophysics and magnetic petrology: aids to geologic interpretation of magnetic surveys. *AGSO J Aust Geol Geophys* 17:83–103
- Clark D (1999) Magnetic petrology of igneous intrusions: implications for exploration and magnetic interpretation. *Explor Geophys* 30:5–26
- Clark D, Lackie M (2003) Palaeomagnetism of the Early Permian Mount Leyshon Intrusive Complex and Tuckers Igneous Complex, North Queensland, Australia. *Geophys J Int* 153(3):523–547. doi:10.1046/j.1365-246x.2003.01907.x
- Clark D, Schmidt P (2001) Petrophysical properties of the Goonumbla volcanic complex, NSW: implications for magnetic and gravity signatures of porphyry Cu-Au mineralization. *Explor Geophys* 32:171–175
- Clark D, Schmidt P, Coward D, Huddleston M (1998) Remote determination of magnetic properties and improved drill targeting of magnetic anomaly sources by Differential Vector Magnetometry (DVM). *Explor Geophys* 29:312–319

- Clark D, Geuna S, Schmidt P (2004) Predictive magnetic exploration models for porphyry, epithermal, and iron oxide copper-gold deposits: implications for exploration, P700 Final Report, AMIRA International Ltd.
- Clem T, Overway D, Purpura J, Bono J, Koch R, Rozen J, Keefe G, Willen S, Mohling R (2001) High-Tc SQUID gradiometer for mobile magnetic anomaly detection. *IEEE Trans Appl. Supercond* 11:871–875
- Cowan D, Cooper G (2005) Enhancement of magnetic signatures of impact craters modeling and petrophysics. In: Kenkmann T, Hörz F, Deutsch A (eds) Large meteorite impacts III, Geological Society of America Boulder, Colorado, Special Paper 384, pp 51–65
- de Castro DL, de Oliveira DC, Gomes Castelo Branco RM (2007) On the tectonics of the Neocomian Rio do Peixe Rift Basin, NE Brazil: lessons from gravity, magnetics, and radiometric data. *J South Am Earth Sci* 24(2–4):184–202. doi:10.1016/j.jsames.2007.04.001
- Drenth BJ, Finn CA (2007) Aeromagnetic mapping of the structure of Pine Canyon caldera and Chisos mountains intrusion, Big Bend National Park, Texas. *Geol Soc Am Bull* 119(11–12):1521–1534
- Dunlop D (2005) Planetary science—Magnetic impact craters. *Nature* 435(7039):156–57. doi:10.1038/435156a
- Esdale D, Pridmore D, Coggon J, Muir P, William P, Fritz F (2003) Olympic dam copper-uranium-gold-silver-rare earth element deposit, South Australia: a geophysical case history. In: Dentith MC (ed) Geophysical signatures of South Australian mineral deposits, Centre for Global Metallogeny, University of Western Australia, Publication 31, pp 147–168
- Espinosa-Cardena JM, Campos-Enriquez JO (2008) Curie point depth from spectral analysis of aeromagnetic data from Cerro Prieto geothermal area, Baja California, Mexico. *J Volcanol Geothermal Res* 176(4):601–609. doi:10.1016/j.jvolgeores.2008.04.014
- Feebrey C, Hishida H, Yoshioka K, Nakayama K (1998) Geophysical expression of low sulphidation epithermal Au-Ag deposits and exploration implications-examples from the Hokusatsu region of SW Kyushu, Japan. *Resour Geol* 48:75–86
- Ferraccioli F, Armadillo E, Jordan T, Bozzo E, Corr H (2009a) Aeromagnetic exploration over the East Antarctic ice sheet: a new view of the Wilkes Subglacial Basin. *Tectonophysics* 478(1–2, Sp. Iss. SI):62–77. doi:10.1016/j.tecto.2009.03.013, General Assembly of the International-Association-of-Geodesy/24th General Assembly of the International-Union-of-Geodesy-and-Geophysics, Perugia, Italy, Jul 02–13, 2007
- Ferraccioli F, Armadillo E, Zunino A, Bozzo E, Rocchi S, Armenti P (2009b) Magmatic and tectonic patterns over the northern Victoria land sector of the transantarctic mountains from new aeromagnetic imaging. *Tectonophysics* 478(1–2, Sp. Iss. SI):43–61. doi:10.1016/j.tecto.2008.11.028, General Assembly of the International-Association-of-Geodesy/24th General Assembly of the International-Union-of-Geodesy-and-Geophysics, Perugia, Italy, Jul 02–13, 2007
- Ferré E, Maes S, Butak K (2009) The magnetic stratification of layered mafic intrusions: Natural examples and numerical models. *Lithos* 111:83–94
- Force E, Dickinson W, Hagstrum J (1995) Tilting history of the San Manuel-Kalamazoo porphyry system, southeastern Arizona. *Econ Geol* 90:67–80
- Frey H (1982) MAGSAT Scalar anomaly distribution-The global perspective. *Geophys Res Lett* 9(4):277–280
- Friis-Christensen E, Lühr H, Hulot G, Haegmans R, Purucker M (2009) Geomagnetic Research from Space. *Eos Trans Am Geophys Union* 90(25):213–214
- Gattacceca J, Berthe L, Boustie M, Vadeboin F, Rochette P, De Resseguier T (2008) On the efficiency of shock magnetization processes. *Phys Earth Planetary Inter* 166(1–2):1–10. doi:10.1016/j.pepi.2007.09.005
- Gee J, Kent D (2007) Source of Oceanic Magnetic Anomalies and the Geomagnetic Polarity Timescale. In: Kono M (ed) *Geomagnetism, treatise of geophysics* Amsterdam, vol 5, Elsevier, 5.12, pp 455–508
- Geissman J, Van der Voo R, KL Howard (1982) A paleomagnetic study of the structural deformation in the Yerington district, Nevada. *Am J Sci* 282:1042–1109
- Gilder S, LeGoff M, Chervin J, Peyronneau J (2004) Magnetic properties of single and multi-domain magnetite under pressures from 0 to 6 GPa. *Geophys Res Lett* 31(10). doi:10.1029/2004GL019844
- Gilder SA, Le Goff M (2008) Systematic pressure enhancement of titanomagnetite magnetization. *Geophys Res Lett* 35(10). doi:10.1029/2008GL033325
- Graham K (1961) The re-magnetization of a surface outcrop by lightning currents. *Geophys J Royal Astronom Soc* 6(1): 85–102
- Grant F (1984) Aeromagnetism, Geology, and ore environments, I. Magnetite in igneous, sedimentary, and metamorphic rocks: an overview. *Geoexploration* 23:303–333
- Grauch VJS, Hudson MR (2007) Guides to understanding the aeromagnetic expression of faults in sedimentary basins: lessons learned from the central Rio Grande rift, New Mexico. *Geosphere* 3(6):596–623. doi:10.1130/GES00128.1
- Grieve RAF, Pilkington M (1996) The signature of terrestrial impacts. *J Aust Geol Geophys* 16:399–420
- Gubbins D, Herrero-Bervera E (eds) (2007) *Encyclopedia of geomagnetism and paleomagnetism*, Springer, The Netherlands
- Guilbert J (1995) Geology, alteration, mineralization and genesis of the Bajo de la Alumbrera porphyry copper-gold deposit, Catamarca Province, Argentina. In: Pierce FW, Bolm JG (eds) *Porphyry copper deposits of the American Cordillera*, Arizona Geological Society Digest 20, pp 646–656
- Gunn P (1997) Regional magnetic and gravity responses of extensional sedimentary basins. *Agso J Aust Geol Geophys* 17(2):115–131
- Gunn P, Mackey T, Meixner A (2009) Magnetic exploration. Technical report Pacific Islands Applied Geoscience Commission, SOPAC Technical Bulletin 11
- Hamoudi M, Thébault E, Lesur V, Mandea M (2007) GeoForschungsZentrum Anomaly Magnetic Map (GAMMA): a candidate model for the world digital magnetic anomaly map. *Geochem Geophys Geosyst* 10. doi:10.1029/2007GC001638
- Haynes D (2000) Iron oxide copper(-gold) deposits: their position in the ore deposit spectrum and modes of origin. In: Porter TM (ed) *Hydrothermal iron oxide copper-gold and related deposits: a global perspective*, vol 1. PGC Publishing, Adelaide, pp 71–90
- Hemant K, Thébault E, Mandea M, Ravat D, Maus S (2007) Magnetic anomaly map of the world: merging satellite,

- airborne, marine and ground-based data. *Earth Planetary Sci Lett* 260:56–71
- Hildenbrand T, Berger B, Jachens R, Ludington S (2000) Regional crustal structures and their relationship to the distribution of ore deposits in the western United States, based on magnetic and gravity data. *Econ Geol* 95:1583–1603
- Hinze W, Von Frese R, Ravat D (1991) Mean magnetic contrasts between oceans and continents. *Tectonophysics* 192(1–2): 117–127. doi:10.1016/0040-1951(91)90250-V
- Hitzman M, Oreskes N, MT Einaudi (1992) Geological characteristics and tectonic setting of proterozoic iron oxide (Cu-U-Au-REE) deposits. *Precambrian Res* 1:1
- Humphrey K, Horton T, Keene M (2005) Detection of mobile targets from a moving platform using an actively shielded, adaptively balanced SQUID gradiometer. *IEEE Trans Appl Supercond* 15(2):753–756
- Hyndman R, Peacock S (2003) Serpentinization of the forearc mantle. *Earth Planetary Sci Lett* 212(3–4):417–432. doi:10.1016/S0012-821X(03)00263-2
- Irvine R, Smith M (1990) Geophysical exploration for epithermal gold systems. *J Geochem Explor* 36:375–412
- Jessel M (2001) Three-dimensional geological modeling of potential-field data. *Comput Geosci* 27:455–465
- Keenan T, Young J, Foley C, Du J (2010) A high-Tc flip-chip SQUID gradiometer for mobile underwater magnetic sensing. *Supercond Sci Technol* 23(025,029):7pp
- Kirby S, Engdahl E, Denlinger R (1996) Intermediate-depth intraslab earthquakes and arc volcanism as physical expressions of crustal and uppermost mantle metamorphism in subducting slabs. In: Bebout GE et al. (eds) *Subduction: top to bottom*, American Geophysical Union Geophysical Monograph 96, pp 195–214
- Korhonen J, et al. (2007) Magnetic anomaly map of the world, and associated DVD, commission for the geological map of the world, UNESCO, Paris, France, Scale:1:50,000,000
- Langlais B, Lesur V, Purucker M, Connerney J, Manda M (2010) Crustal magnetic fields of terrestrial planets. *Space Sci Rev*. doi:10.1007/s11214-009-9557-y, 152:223–249
- Leslie K, Blay K, Clark D, Schmidt P, Tilbrook D, Bick M, Foley C (2007) Helicopter trial of magnetic tensor gradiometer. In: ASEG 19th International Conference, Perth, Australia
- Lillis RJ, Frey HV, Manga M, Mitchell DL, Lin RP, MH Acuña, Bougher SW (2008) An improved crustal magnetic field map of Mars from electron reflectometry: highland volcano magmatic history and the end of the martian dynamo. *Icarus* 194(2):575–596. doi:10.1016/j.icarus.2007.09.032
- Lillis RJ, Purucker ME, Louzada HJS, Stewart-Mukhopadhyay K, Manga M, Frey H (2010) Study of impact demagnetization on Mars using Monte Carlo modeling and multiple altitude data. *J Geophys Res Planet*. 115, E07007, doi:10.1029/2009JE003556
- Lindsay D, Zentilli M, Rojas de la Rivera J (1995) Evolution of an active ductile to brittle shear system controlling mineralization at the Chuquicamata porphyry copper deposit, northern Chile. *Int Geol Rev* 37:945–958
- Louzada KL, Weiss BP, Maloof AC, Stewart ST, Swanson-Hysell NL, Soule SA (2008) Paleomagnetism of Lonar impact crater, India. *Earth Planetary Sci Lett* 275(3–4):308–319. doi:10.1016/j.epsl.2008.08.025
- Lowell J (1968) Geology of the Kalamazoo orebody, San Manuel district, Arizona. *Econ Geol* 63:645–654
- Lowell J, Guilbert J (1970) Lateral and vertical alteration-mineralization zoning in porphyry copper deposits. *Econ Geol* 65:373–408
- Lum J, Clark A, Coleman P (1991) Gold potential of the southwest Pacific: Papua New Guinea, Solomon Islands, Vanuatu, and Fiji, Technical report, East-West Center, Honolulu
- MacDonald G, Arnold L (1994) Geological and geochemical zoning of the Grasberg Igneous complex, Irian Java, Indonesia. *J Geochem Explor* 50:179–202
- Maden N (2009) Crustal Thermal Properties of the Central Pontides (Northern Turkey) deduced from spectral analysis of magnetic data. *Turkish J Earth Sci* 18(3):383–392. doi:10.3906/yer-0803-7
- Maia M, Dymant J, Jouannetaud D (2005) Constraints on age and construction process of the Foundation chain submarine volcanoes from magnetic modeling. *Earth Planet Sci Lett* 235(1–2):183–199. doi:10.1016/j.epsl.2005.02.044
- Manda M, Purucker M (2005) Observing, modeling, and interpreting magnetic fields of the solid Earth. *Surv Geophys* 26(4):415–459. doi:10.1007/s10712-005-3857-x
- Manea M, Manea VC (2008) On the origin of El Chichon volcano and subduction of Tehuantepec ridge: a geodynamical perspective. *J Volcanol Geotherm Res* 175(4, Sp. Iss. SI):459–471. doi:10.1016/j.jvolgeores.2008.02.028
- Maus S, Gordon D, Fairhead D (1997) Curie-temperature depth estimation using a self-similar magnetization model. *Geophys J Int* 129(1):163–168
- Maus S, Luehr H, Rother M, Hemant K, Balasis G, Ritter P, Stolle C (2007a) Fifth-generation lithospheric magnetic field model from CHAMP satellite measurements. *Geochem Geophys Geosyst* 8. doi:10.1029/2006GC001521
- Maus S, Sazonova T, Hemant K, Fairhead J, Ravat D (2007b) National geophysical data center candidate for the world digital magnetic anomaly map. *Geochem Geophys Geosyst* 8(6). doi:10.1029/2007GC001643
- McDowell F, McMahon T, Warren P, Cloos M (1996) Pliocene Cu-Aubearing igneous intrusions of the Gunung Bijih (Ertsberg) district, Irian Java, Indonesia: K-Ar geochronology. *J Geol* 104:327–340
- McEnroe S, Langenhorst F, Robinson P, Bromiley G, Shaw C (2004) What is magnetic in the lower crust? *Earth Planet Sci Lett* 226(1–2):175–192. doi:10.1016/j.epsl.2004.07.020
- McEnroe S, Brown L, Robinson P (2009a) Remanent and induced magnetic anomalies over a layered intrusion: Effects from crystal fractionation and magma recharge. *Tectonophysics* 478:119–134
- McEnroe S, Fabian K, Robinson P, Gaina C, Brown LL (2009b) Crustal magnetism, lamellar magnetism and rocks that remember. *Elements* 5(4):241–246. doi:10.2113/gselements.5.4.241
- Melosh H (1989) *Impact cratering: a geologic process*, Oxford University Press, New York, NY
- Muundjua M, Hart RJ, Gilder SA, Carporzen L, Galdeano A (2007) Magnetic imaging of the Vredefort impact crater, South Africa. *Earth Planetary Sci Lett* 261(3–4):456–468. doi:10.1016/j.epsl.2007.07.044
- Muundjua M, Galdeano A, Carporzen L, Gilder SA, Hart RJ, Andreoli MAG, Tredoux M (2008) Reply to comment by Reimold WU, Gibson RL, Henkel H on Muundjua et al. (2007), Magnetic imaging of the Vredefort impact crater, South Africa, *EPSL* 261, pp 456–468

- Discussion. *Earth Planet Sci Lett* 273(3–4):397–399. doi:10.1016/j.epsl.2008.06.044
- Nabighian M, Grauch V, Hansen R, LaFehr T, Li Y, Peirce J, Phillips J, Ruder M (2005) 75th Anniversary—The historical development of the magnetic method in exploration. *Geophys* 70(6):33ND–61ND. doi:10.1190/1.2133784
- Oleskevich D, Hyndman R, Wang K (1999) The updip and downdip limits to great subduction earthquakes: thermal and structural models of Cascadia, south Alaska, SW Japan, and Chile. *J Geophys Res Solid Earth* 104(B7):14,965–14,991
- Parker R (1991) A theory of Ideal bodies for Seamount magnetism. *J Geophys Res Solid Earth* 96(B10)
- Parker R (2003) Ideal bodies for Mars magnetic. *J Geophys Res Planet* 108(E1). doi:10.1029/2001JE001760
- Peacock S, Wang K, McMahon A (2002) Thermal structure and metamorphism of subducting oceanic crust: insight into Cascadia intraslab earthquakes and processes, and earthquake hazards, Open-file Report 02-328, 17–24, U.S. Geological Survey
- Pedersen L, Rasmussen T (1990) The gradient tensor of potential field anomalies: some implications on data collection and data processing of maps. *Geophys* 55:1558–1566
- Phillips J (1997) Potential-field geophysical software for the PC-version 2.2, Open-file Report 97-725, U.S. Geological Survey
- Pilkington M, Hildebrand A (2003) Transient and disruption cavity dimensions of complex terrestrial impact structures derived from magnetic data. *Geophys Res Lett* 30(21). doi:10.1029/2003GL018294
- Potter D (1996) What makes Grasberg anomalous, implications for future exploration. In: Porphyry related copper and gold deposits of the Asia Pacific region, Australian Mineral Foundation, pp 10.1–10.13
- Prutkin I, Saleh A (2009) Gravity and magnetic data inversion for 3D topography of the Moho discontinuity in the northern Red Sea area, Egypt. *J Geodynam* 47(5):237–245. doi:10.1016/j.jog.2008.12.001
- Purucker M, SerpentTeam M (2010) Magnetic signatures of serpentinized mantle and mesoscale variability along the Alaska/Aleutian subduction zone, in Abstract book of the European Geoscience Union, Vienna, Austria
- Purucker M, Whaler K (2007) Crustal Magnetism. In: Kono M (ed) *Geomagnetism, Treatise of Geophysics*, vol 5, Chapter 6. Elsevier, Amsterdam, pp 195–236
- Purucker M, Sabaka T, Le G, Slavin JA, Strangeway RJ, Busby C (2007) Magnetic field gradients from the ST-5 constellation: Improving magnetic and thermal models of the lithosphere. *Geophys Res Lett* 34(24). L24306 doi:10.1029/2007GL031739
- Purucker M, Olsen N, Sabaka T, HR (2009a) Geomagnetism mission concepts after Swarm, in Abstract book of the Int. Assoc. Geomag. Aeronom. 11th Scientific Assembly, Sopron, Hungary, pp 105
- Purucker ME, Sabaka TJ, Solomon SC, Anderson BJ, Korh H, Zuber MT, Neumann GA (2009b) Mercury's internal magnetic field: Constraints on large- and small-scale fields of crustal origin. *Earth Planet Sci Lett* 285(3–4, Sp. Iss. SI):340–346. doi:10.1016/j.epsl.2008.12.017
- Quesnel Y, Catalan M, Ishihara T (2009) A new global marine magnetic anomaly data set. *J Geophys Res Solid Earth* 114(B04106). doi:10.1029/2008JB006144
- Rabeh T, Miranda M (2008) A tectonic model of the Sinai Peninsula based on magnetic data. *J Geophys Eng* 5(4): 469–479. doi:10.1088/1742-2132/5/4/010
- Rajaram M, Anand SP, Hemant K, Purucker ME (2009) Curie isotherm map of Indian subcontinent from satellite and aeromagnetic data. *Earth Planetary Sci Lett* 281(3–4):147–158. doi:10.1016/j.epsl.2009.02.013
- Ranganai RT, Ebinger CJ (2008) Aeromagnetic and Landsat TM structural interpretation for identifying regional groundwater exploration targets, south-central Zimbabwe Craton. *J Appl Geophys* 65(2):73–83. doi:10.1016/j.jappgeo.2008.05.009
- Ravat D, et al. (2009) A preliminary, full spectrum magnetic anomaly grid of the United States with improved long wavelengths for studying continental dynamics: a website for distribution of data, Open-file Report 2009-1258, U.S. Geological Survey
- Ravat D, Pignatelli A, Nicolosi I, Chiappini M (2007) A study of spectral methods of estimating the depth to the bottom of magnetic sources from near-surface magnetic anomaly data. *Geophys J Int* 169(2):421–434. doi:10.1111/j.1365-246X.2007.03305.x
- Reeves C (2007) The role of airborne geophysical reconnaissance in exploration geosciences. *First Break* 19(9):501–508
- Reimold WU, Gibson RL, Henkel H (2008) Scientific comment on In: Muundjua et al., 2007: magnetic imaging of the Vredefort impact crater, South Africa, *EPSL* 261, 456–468 Discussion. *Earth Planet Sci Lett* 273(3–4): 393–396. doi:10.1016/j.epsl.2008.06.046
- Robinson D, et al. (2008) Advancing process-based watershed hydrological research using near-surface geophysics: a vision for, and review of, electrical and magnetic geophysical methods. *Hydrol Process* 22:3604–3635
- Ross HE, Blakely RJ, Zoback MD (2006) Testing the use of aeromagnetic data for the determination of Curie depth in California. *Geophys* 71(5):L51–L59. doi:10.1190/1.2335572
- Saadi NM, Watanabe K, Imai A, Saibi H (2008) Integrating potential fields with remote sensing data for geological investigations in the Eljufra area of Libya. *Earth Planets Space* 60(6):539–547
- Sandrin A, Elming S (2006) Geophysical and petrophysical study of an iron oxide copper gold deposit in northern Sweden. *Ore Geol Rev* 29:1–18
- Sandrin A, Berggren R, Elming S (2007) Geophysical targeting of Feoxide Cu-(Au) deposits west of Kiruna, Sweden. *J Appl Geophys* 61:92–101
- Schmidt P, Clark D (2006) The magnetic gradient tensor: its properties and uses in source characterization. *Leading Edge* 25(1):75–78
- Schmidt P, Clark D, Logan K (1997) Paleomagnetism, magnetic petrophysics and magnetic signature of the Porgera Intrusive Complex, Papua New Guinea. *Explor Geophys* 28:276–280
- Schmidt PW, McEnroe SA, Clark DA, Robinson P (2007) Magnetic properties and potential field modeling of the Peculiar Knob metamorphosed iron formation, South Australia: an analog for the source of the intense Martian magnetic anomalies? *J Geophys Res Solid Earth* 112(B3). doi:10.1029/2006JB004495
- Schubert G (ed) (2007) *Treatise on geophysics*. Elsevier, Amsterdam
- Shepherd T, Bamber J, Ferraccioli F (2006) Subglacial geology in coats land, East Antarctica, revealed by airborne magnetics

- and radar sounding. *Earth Planetary Sci Lett* 244(1–2): 323–335. doi:10.1016/j.epsl.2006.01.068
- Sherrod BL, Blakely RJ, Weaver CS, Kelsey HM, Barnett E, Liberty L, Meagher KL, Pape K (2008) Finding concealed active faults: extending the southern Whidbey Island fault across the Puget Lowland, Washington. *J Geophys Res Solid Earth* 113(B5). doi:10.1029/2007JB005060
- Sillitoe R (2000) Gold-rich porphyry deposits: descriptive and genetic models and their role in exploration and discovery. In: Hagemann, SG, Brown PE (eds) *Gold in 2000*, Society of Economic Geologists, Littleton, Colorado, vol. 13. *Reviews of Economic Geology*, pp 315–345
- Singh K, Okuma S, Special issue—Magnetic anomalies: tectonophysics. *Tectonophysics* 478:1–142
- Smith R (2002) Geophysics of iron oxide copper-gold deposits. In: Porter TM (ed) *Hydrothermal Iron Oxide Copper-Gold and related deposits: a global perspective*, vol 2. PGC Publishing, Adelaide, pp 123–136
- Spector A, Grant F (1970) Statistical models for interpreting aeromagnetic data. *Geophysics* 35(2):293–302
- Spray J, Butler H, Thompson L (2004) Tectonic influences on the morphometry of the Sudbury impact structure: Implications for terrestrial cratering and modeling. *Meteoritics Planetary Sci* 39(2):287–301
- Stampolidis A, Kane I, Tsokas G, Tsourlos P (2005) Curie point depths of Albania inferred from ground total field magnetic data. *Surveys Geophys* 26(4):461–480. doi:10.1007/s10712-005-7886-2
- Stolz R, Chwala A, Zakosarenko V, Schulz M, Fritzsche L, Meyer H (2006) SQUID technology for geophysical exploration. In: SEG Expanded abstracts 25, pp 894–898
- Sunderland A, Golden H, McRae W, Varyaskin A, Blair D (2009) Results from a novel direct magnetic gradiometer. *Explor Geophys* 40:222–226
- Syberg F (1972) A Fourier method for the regional-residual of potential fields. *Geophys Prospect* 20:47–75
- ten Brink US, Rybakov M, Al-Zoubi AS, Rotstein Y (2007) Magnetic character of a large continental transform: an aeromagnetic survey of the dead sea fault. *Geochem Geophys Geosyst* 8. doi:10.1029/2007GC001582
- Thébaud E, Purucker M, Whaler K, Langlais B, Sabaka T, The magnetic field of the Earth's lithosphere. *Space Sci Rev* in press
- Trifonova P, Zhelev Z, Petrova T, Bojadgieva K (2009) Curie point depths of Bulgarian territory inferred from geomagnetic observations and its correlation with regional thermal structure and seismicity. *Tectonophysics* 473(3–4):362–374. doi:10.1016/j.tecto.2009.03.014
- Ugalde H, Artemieva N, Milkereit B (2005) Magnetization on impact structures—Constraints from numerical modeling and petrophysics. In: Kenkmann T, Hörz, F, Deutsch A (eds) *Large meteorite impacts III*, Geological Society of America Special Paper 384, pp 25–42
- Wall V, Gow P (1995) Some copper-gold ore-forming systems: iron(ic) connections. In: Clark AH (ed) *Giant Ore Deposits-II, Controls on the Scale or Orogenic Magmatic-Hydrothermal Mineralization*. Proceedings of the Second Giant Ore Deposits Workshop, Kingston, Ontario, Canada, pp 557–582
- Wessel P, Müller R (2007) Plate tectonics. In: Watts AB (ed) *Crust and lithosphere dynamics*, Treatise of Geophysics, vol 6. Elsevier, Amsterdam, pp 6.02, 49–98
- Wiegert R, Oeschger J, Tuovila E (2007) Demonstration of a novel manportable magnetic STAR technology for real time localization of unexploded ordnance, in Proceedings of MTS/IEEE Oceans 2007
- Wilkins J, Heidrick T (1995) Post Laramide extension and rotation of porphyry copper deposits, southwestern United States. In: Pierce FW, Bolm JG (eds) *Porphyry copper deposits of the American Cordillera*, Arizona Geological Society Digest 20, pp 109–127
- Xu-Zhi H, Ming-Jie X, Xiao-An X, Liang-Shu W, Qing-Long Z, Shao-Wen L, Guo-Ai X, Chang-Ge F (2006) A characteristic analysis of aeromagnetic anomalies and Curie point isotherms in Northeast China. *Chinese J Geophys Chinese Edn* 49(6):1674–1681